STRESS TRANSFER DUE TO CREEP IN A SATURATED CLAY

Thesis for the Degree of M. S.
MICHIGAN STATE UNIVERSITY
Frank J. Holliday
1963

ABSTRACT

STRESS TRANSFER DUE TO CREEP
IN A SATURATED CLAY

by Frank J. Holliday

An experimental study was made to determine the behavior of friction and cohesion in a clay soil during creep. Creep-CFS tests were used to determine cohesion and friction at the end of different periods of elapsed creep time. The results were compared with the stress transfer curves calculated from Creep tests.

The increase in friction and decrease in cohesion with creep time measured with the Creep-CFS test were similar to the increase in frictional resistance and decrease in cohesive resistance computed from the Creep test. The behavior of the frictional and cohesive components can be represented by the elastic and viscous elements of the Kelvin rheological model.

STRESS TRANSFER DUE TO CREEP IN A SATURATED CLAY

by

Frank J. Holliday

A THESIS

Submitted to
the College of Engineering of
Michigan State University
in partial fulfillment of the requirements
for the degree of

MASTER OF SCIENCE

Department of Civil Engineering

1963

ACKNOWLEDGEMENTS

The writer is indebted to Dr. T. H. Wu, Department of Civil Engineering, for his guidance, assistance, and encouragement throughout the writer's Master's Degree program. Thanks are expressed to Dr. O. B. Andersland for time spent with the writer during Dr. Wu's absence and to the writer's colleagues, A. K. Loh and R. W. Christensen, for assistance in and out of the laboratory.

The writer wishes to express his appreciation to the National Science Foundation for the Graduate Research Assistantship which made graduate work at Michigan State University possible.

TABLE OF CONTENTS

LIST OF TABLES

LIST OF FIGURES

Figure Page

NOTATION

σ = Axial stress

ϵ = Axial strain

E = Constant associated with spring

$\dot{\epsilon}$ = Strain rate

α = Constant associated with dashpot

τ = Maximum shear stress

γ = Maximum shear strain

G = Constant associated with spring

ζ = Constant associated with dashpot

t = Time

τ_G = Shear stress in spring

τ_ζ = Shear stress in dashpot

K = Constant maximum shear stress

τ_ϕ = Shear stress associated with friction

τ_c = Shear stress associated with cohesion

$(\sigma_1 - \sigma_3)$ = Principal stress difference

ϕ' = Friction

c' = Cohesion

$\bar{\sigma}_1$ = Effective axial stress

$\bar{\sigma}_3$ = Effective radial stress

γ_F = Shear strain at time of negligible strain rate

τ_T = Threshold value of shear stress

K = Shear stress due to creep load

I INTRODUCTION

Soil engineers have had the problem of creep during sustained loading of clay soils for many years. Buisman (1936) noted that results of long duration tests on peat and clay showed total deformation resulting from a combination of deformation due to "direct load effect" and a "time dependent" deformation. Buisman observed "Continuously decreasing deformation" in the consolidation process and termed this phenomenon the "secular" effect. Geuze (1948) later reported that Buisman's "secular law" was followed during the consolidation process and at low values of shear stress by cohesive soils.

Casagrande and Wilson (1950) presented data from two types of tests (creep strength tests and long time compression tests) showing clearly the time effects on deformation and strength of clays. The loss of strength with time observed in saturated clays could account for slides on slopes which failed after standing for many years. Geuze (1953) and Haefeli (1953) presented field observations of soil failures after excessive creep. Terzaghi (1953) pointed out that little was known about creep and stated that much research and study was needed in this area.

The recognition of the creep problem led to application of the theories of rheology in an attempt to describe mathematically the creep in soils. Vialov and Skibitsy (1957) (1961), Geuze (1953), Geuze and Tan (1954), Haefeli (1953)and Schiffman (1959) presented papers on the rheological analysis of deformation. Murayama and

Shibata (1961) proposed a four element rheologic model to explain the viscosity, elasticity and internal resistance of clays.

Rowe (1957) presented a hypothesis suggesting that "creep will lead to a gradual increase in the pressure on structures which resist movement, the ultimate pressure being that due to soil having only friction." This suggests that as creep progresses the value of cohesion should decrease to a small value or zero and values of friction should increase. This hypothesis was substantiated by Schmertmann and Hall (1961), Wu, Douglas, and Goughnour (1962) and Bea (1963). They showed that cohesion and friction during creep followed time dependent relationships that are visco-elastic in nature.

The soil parameters friction and cohesion are defined according to Schmertmann and Osterberg (1960) as follows:

Friction - The angle of internal friction, at any strain, is the angle whose tangent is the ratio of the change in shear stress to the change in normal intergranular stress occurring on the plane of Mohr envelope tangency at that strain, during a stress change occurring without significant change in soil structure.

Cohesion - The cohesion of a soil, at any strain, is the shear stress developed on the plane of Mohr envelope tangency at that strain, if the intergranular stress on that plane could be reduced to zero without significant change in soil structure.

It is the objective of this research to study the behavior of friction and cohesion of a clay soil during creep as elastic and viscous resistance components of the material to deformation. One of the simplest rheologic models of visco-elastic behavior is the Kelvin model. Although the Kelvin model does not completely describe the complex nature of creep, its simplicity is an advantage in establishing a first approximation of the action of cohesion and friction during deformation.

II APPLICATION OF RHEOLOGY

2.1 Elastic and Viscous Elements

The rheologic behavior of materials is represented by visco-elastic models consisting of dashpots and springs in series or parallel. The elastic solid is represented by the spring and the viscous fluid is represented by the dashpot. Figure 1 shows the schematic of a spring and Figure 2 shows the schematic of a dashpot.

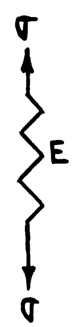

Figure 1 - Spring or Elastic Element

The equation for linear elastic behavior represented by the spring in Figure 1 is

$$\sigma = E\,\epsilon$$

Where

σ = Axial stress,

ϵ = Axial strain,

E = Constant associated with spring.

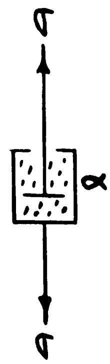

Figure 2 - Dashpot or Viscous Element

The equation for viscous fluid behavior represented by the dashpot in Figure 2 is

$$\sigma = \alpha \dot{\epsilon}$$

Where

σ = Axial stress,

$\dot{\epsilon}$ = Axial strain rate,

α = Constant associated with dashpot.

Application of this concept of the rheologic model to soil mechanics requires the assumptions of continuity and homogeneity. Under the condition of no volume change all deformations are the result of shear stresses. The deformations under a set of principal stresses can be correlated with the shear stress.

By applying the above conditions the equations for the elastic element and viscous element become respectively:

$$\tau = G \gamma \qquad (2.1\text{-}1)$$

$$\tau = \eta \frac{d\gamma}{dt} \qquad (2.1\text{-}2)$$

Where

τ = Maximum shear stress,

γ = Maximum shear strain,

G = Constant associated with spring (shear modulus),

η = Constant associated with dashpot (viscosity),

t = time.

2.2 Maxwell and Kelvin Models

Series arrangement of the spring and dashpot is called the Maxwell model. The Maxwell model's characteristic shear strain versus time curve is shown in Figure 3 where τ/G is equal to the instantaneous shear strain in the elastic element under a constant shear stress condition.

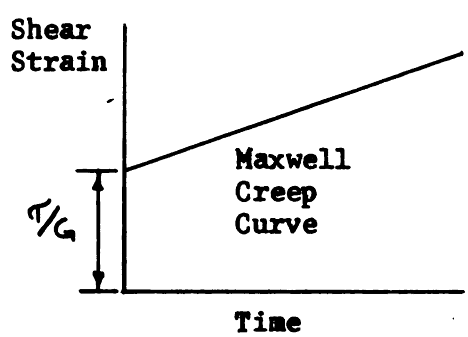

Figure 3 - Shear Strain Versus Time Curve for Maxwell Model

The parallel arrangement of a spring and a dashpot is called the Kelvin (or Voigt) model. Figure 4 shows a schematic drawing of the Kelvin model.

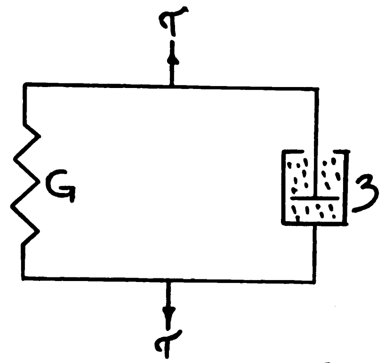

Figure 4 - Kelvin Model

Since the strain in each element of the Kelvin model is equal to the total strain of the model and the sum of the shear stress in each element is equal to the total shear stress on the model, the following equations apply:

$$\tau_G = G\gamma$$
$$\tau_\eta = \eta \frac{d\gamma}{dt}$$
$$\tau = \tau_G + \tau_\eta = G\gamma + \eta \frac{d\gamma}{dt} \qquad (2.2\text{-}1)$$

Where

τ_G = Shear stress in spring,

τ_η = Shear stress in dashpot,

γ = Shear strain of model.

Solution of equation (2.2-1) under the condition of constant shear stress τ gives:

$$\gamma = \tau/G\left(1 - e^{-(G/\eta)\,t}\right). \qquad (2.2\text{-}2)$$

Figure 5 shows a plot of equation (2.2-2) where τ/G is equal to the strain in the elastic element at time equal to infinity under a constant shear stress condition.

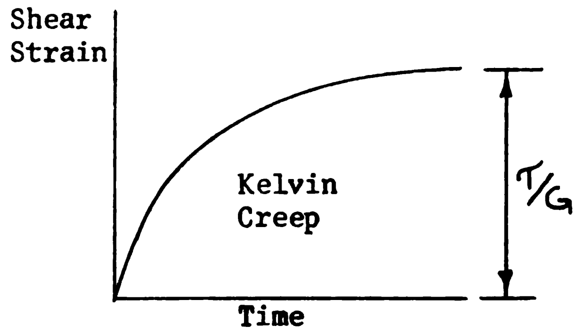

Figure 5 - Shear Strain Versus Time Curve for Kelvin Model

When the Kelvin body is subjected to a constant shear stress there is a stress transfer from the dashpot to the spring. This transfer can be shown by substitution of equation (2.2-2) into equation (2.2-1). The transfer is as follows:

$$\tau = \tau_G + \tau_\eta = K\,(1 - e^{-(G/\eta)\,t}) + K\,e^{-(G/\eta)\,t}$$

Where

K = Constant shearing stress.

The shape of the stress transfer curves are shown in Figure 6.

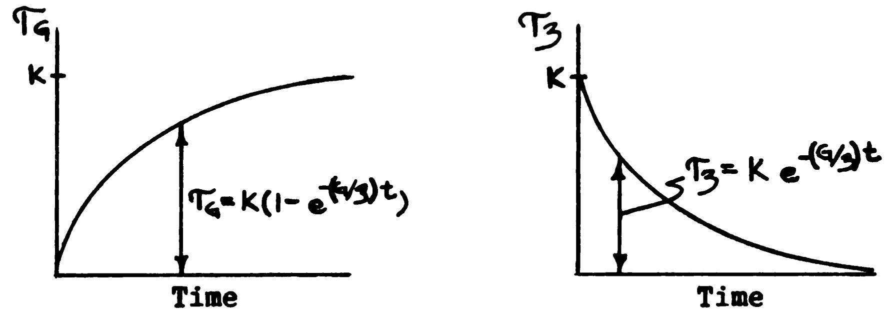

Figure 6 - Stress Transfer Curves for Kelvin Model

2.3 Application of Kelvin Model to Saturated Clay

Figure 3 and Figure 5 show the shape of creep curve described by the Maxwell equation and the Kelvin equation. Curves presented by Casagrande and Wilson (1950), Geuze and Tan (1954), and Wu, Douglas and Goughnor (1962) have shapes similar to the curve in Figure 5. This similarity indicates that the creep in a saturated clay is better represented by a Kelvin model than a Maxwell model.

Wu, Douglas, and Goughnour (1962), and Bea (1963) respectively proposed and substantiated the increase in friction and the decrease in cohesion in a saturated clay soil as creep progressed. This transfer behavior is similar to the transfer behavior of the Kelvin model. Letting the spring represent friction and the dashpot represent the cohesion, expressions for the stress transfer in a saturated clay can be written as:

$$\tau_G = \tau_\phi = G\gamma = K(1 - e^{-(G/\eta)t}) \qquad (2.3\text{-}1)$$

$$\tau_\eta = \tau_c = \eta\frac{d\gamma}{dt} = K\,e^{-(G/\eta)t} \qquad (2.3\text{-}2)$$

$$K = \tau_\phi + \tau_c = G\gamma + \eta\frac{d\gamma}{dt} \qquad (2.3\text{-}3)$$

Where

τ_ϕ = Shear stress associated with friction,

τ_c = Shear stress associated with cohesion,

K = Shear stress due to creep load.

Stress transfer curves have the same shape as those in Figure 6.

III EXPERIMENTAL PROGRAM

3.1 Soil Used

The glacial lake clay used in this investigation was from a site approximately 15 miles south of Sault Ste. Marie, Michigan. This clay was obtained at a depth of about 5 feet below the ground surface. X-ray defraction tests (Dillon 1963) show the soil contains about 50 percent illite, 25 percent vermiculite, 15 percent chlorite, and 10 percent as a combination of montmorillonite, quartz, feldspar, and kaolinite. See Table 1 for index properties.

Table 1 - Properties of Sault Ste. Marie Clay

Air Dry Water Content 2.64%	Liquid Limit 60.5%	Plastic Limit 23.6%
Shrinkage Limit 19.1%	Plasticity Index 36.2%	Specific Gravity 2.79
Clay Fraction 0.60	Silt Fraction 0.40	Activity 0.63

3.2 Sample Preparation

Compacted and consolidated samples were used in this investigation.

The soil prior to compaction was prepared by passing the clay through a muller until it would pass a No. 10 (U. S. Standard) sieve. The air dry water content was determined and distilled water added to obtain a water content from 40 to 45 percent. The clay was thoroughly mixed by hand as water was added, placed in an earthenware crock and stored at about 70 degrees fahrenheit and 100 percent humidity until the water content was uniform throughout.

a) Compacted clay

Two weeks later the clay was removed from the crock and placed by hand in a circular mold with an inside diameter of 11.25 inches and a depth of 6.5 inches.

Figure 7 - Compaction Apparatus

One inch diameter clay balls were placed in layers and pressed together by hand to avoid large voids and achieve continuity of the samples. Sufficient clay was placed in the mold to make a compacted cake about 6 inches in height. After placement in the mold the clay was subjected to a pressure of 1 kilogram per square centimeter for about one hour in a hydraulic testing machine (Figure 7). Next the two halves of the mold were separated, the cake removed, and cut into 21 pieces. Each piece was given 2 coats of wax, wrapped in aluminum foil, given 3 coats of wax, and stored under water until used. Sealing wax used was Gulf Oil Corporation's Petrowax A. Figure 8 shows the scheme used to cut cake.

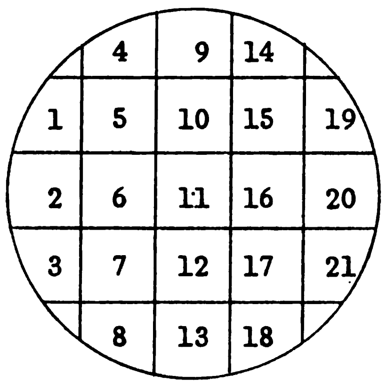

11.25 inch diameter cake
6.0" high
Samples about 2" x 2" x 6"
Scale: 1.0" = 6.0"

Figure 8 - Division of Compacted Cake

b) Consolidated Clay

The consolidated cake was prepared in a consolidometer consisting of 6 inch diameter lucite tubes mounted on a brass base. Porous stones placed on top and bottom of the soil and side drains permitted water drainage. Approximately 6 inches of clay paste at a water content close to the liquid limit was placed in the apparatus and allowed to settle. After settlement the clear liquid above the soil was drawn off and another 6 inches of clay paste added. This procedure was repeated until the soil cake was of desired height. When adding the second 6 inches of clay paste and subsequent lifts, extreme care was taken not to disturb the clay already in the consolidometer.

After settlement was complete the clay was loaded and consolidated. The first load increment was 0.003 kilogram per square centimeter and the increment was doubled until the load totaled 0.36 kilogram per square centimeter. Each increment was left until at least 90 percent consolidation was achieved. The consolidated cake was extruded from the consolidometer, cut into 6 equal, wedge-shaped sections and waxed. After waxing the samples were stored as described above for the compacted samples.

3.3 Triaxial Tests

Triaxial shear tests were used to measure the cohesion and friction. The samples were trimmed to finished dimensions of about 1.4 inches in diameter by 3 inches long. Three wool yarns were placed longitudinally in the center of the sample and 3 paper towel drains 1/4 inch wide by 8 inches long were placed longitudinally around the sample. These drains decreased consolidation time and speeded pore pressure response.

The samples were hydrostatically consolidated under a pressure of 2 kilograms per square centimeter for 24 hours. After consolidation, drainage was stopped and a back pressure of 1.5 kilograms per square centimeter applied to saturate the sample. The back pressure was applied by raising the cell pressure and the pore pressure simultaneously by 0.1 kilogram per square centimeter increments until a pore pressure of 1.5 kilogram per square centimeter was reached. The back pressure was maintained for at least 12 hours.

The saturation of randomly selected samples was checked by measurement of the "B" parameter. (Bishop and Henkel, 1962) The results of a typical "B" parameter test are given in Table 2.

Table 2 - "B" Parameter Test Data

Sample: C-C-CFS-9
Starting Cell Pressure: $\sigma_3 = 3.5$ Kg/cm^2
Starting Pore Pressure: $u = 1.5$ Kg/cm^2

$$B = \frac{\text{change in } u}{\text{change in } \sigma_3}$$

Elapsed Time in Min.	σ_3 Kg/cm^2	u Kg/cm^2	Change in σ_3	Change in u	"B"
0	3.75	1.5	0.25	0.00	-
1	3.75	1.75	0.25	0.25	1
2	3.75	1.75	0.25	0.25	1
5	3.75	1.75	0.25	0.25	1
10	3.75	1.75	0.25	0.25	1
0	4.0	1.75	0.50	0.25	-
1	4.0	2.00	0.50	0.50	1
2	4.0	2.00	0.50	0.50	1
5	4.0	2.00	0.50	0.50	1
10	4.0	2.00	0.50	0.50	1

The three types of tests run on the samples of compacted and consolidated clay were Creep tests, CFS tests, and Creep-CFS tests.

a) Creep Test

The sample was prepared, placed in the triaxial cell, consolidated and back pressured. It was then loaded by dead weights as shown in Figure 9.

The change in area of the sample was small during deformation so the original load on the sample did not need adjustment to keep the stress essentially constant. The sample was allowed to deform

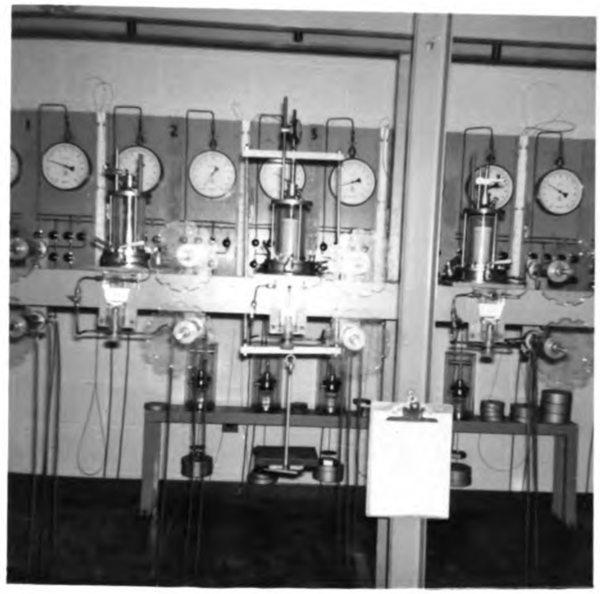

Figure 9 - Creep Test

with no drainage until the strain rate became negligible. Axial strain and pore pressure readings were taken at time intervals beginning with 15 seconds. The time interval was doubled until 12 hours was reached, then a 12 hour increment was used. Axial strain measurements were recorded to nearest 0.001 inch and pore pressure measurements were read to nearest 0.05 kilogram per square centimeter.

b) CFS Test

The CFS test followed the procedure outlined by Schmertmann and Osterberg (1960) with some minor changes due to differences in equipment. The procedure used is outlined below.

After the sample was consolidated and back pressured, the piping system for the triaxial cell was set up as shown in Figure 10.

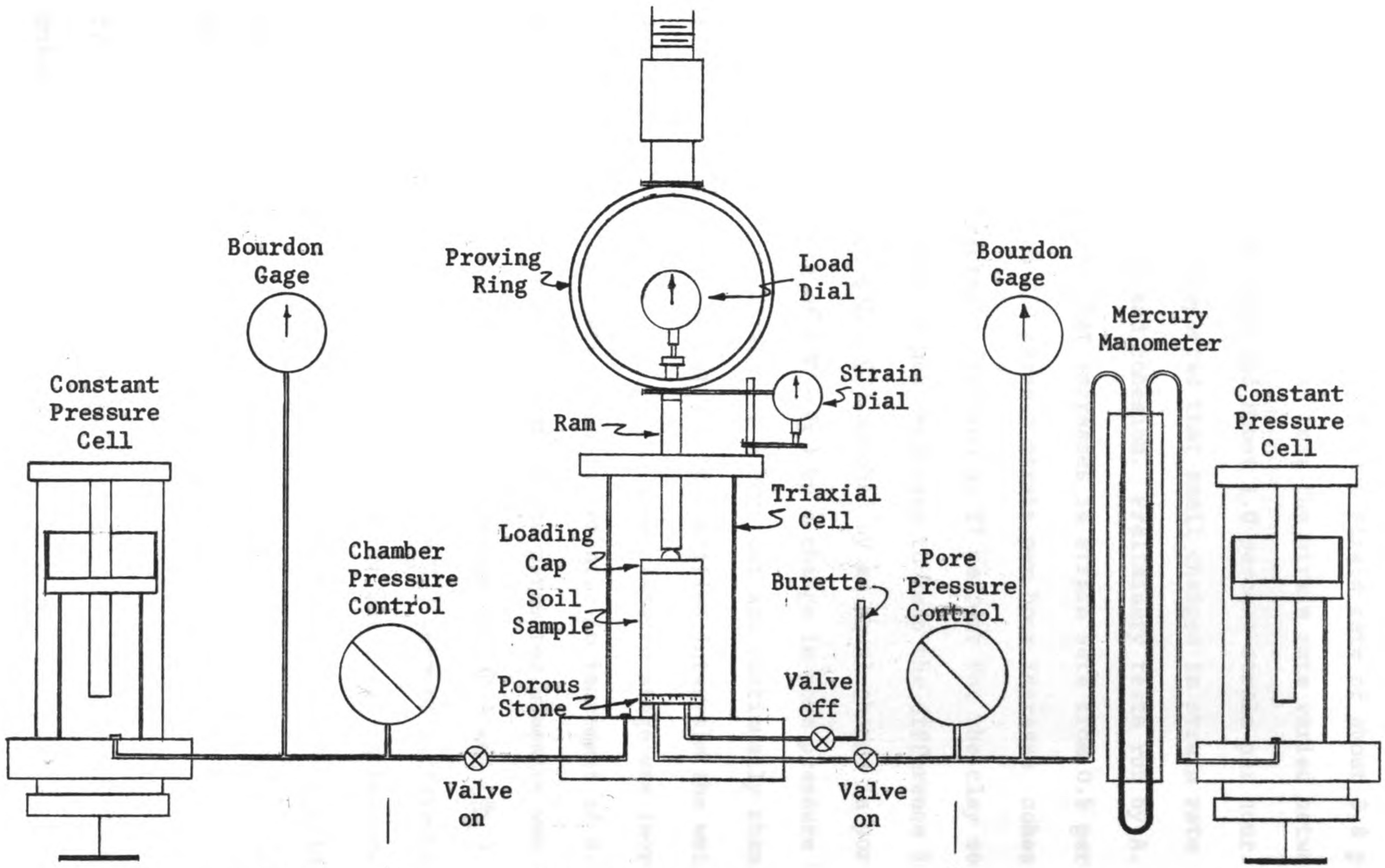

FIGURE 10 - SCHEMATIC DRAWING OF CFS TEST

The test was run at a constant strain rate of about 0.8 percent strain per hour. During the test the strain rate varied between 0.8 percent strain per hour and about 1.0 percent strain per hour. Schmertmann (1962) reported that small changes in strain rate did not affect friction and cohesion. Preliminary tests run by A. K. Loh and the writer show that increases in strain rate from 0.5 percent strain per hour to 1.0 percent strain per hour increase cohesion by 29 percent and decrease friction by 27 percent for the clay soil used.

During the test it was necessary to keep the difference in principal stresses ($\sigma_1 - \sigma_3$) matched by an equal change in pore pressure. Matching of ($\sigma_1 - \sigma_3$) by a change in pore pressure held the effective axial stress ($\bar{\sigma}_1$) constant and continually changed the effective radial stress ($\bar{\sigma}_3$). At specified intervals the weight on the constant pressure cell in the pore pressure stage was increased or decreased by a predetermined increment. An increment of 0.5 kilogram per square centimeter in the porewater pressure was used. This produced an equal and opposite change in ($\bar{\sigma}_1$) and ($\bar{\sigma}_3$). Under the new ($\bar{\sigma}_1$) the deviator stress ($\sigma_1 - \sigma_3$) behaved differently and the pore pressure was adjusted so that it was equal to the new ($\sigma_1 - \sigma_3$). When the matching operation and the weight changing operation were superimposed a ($\sigma_1 - \sigma_3$) versus axial strain curve was obtained for each level of ($\bar{\sigma}_1$).

Using Mohr's circle and the theory of effective stress, the friction (ϕ') and cohesion (c') at various axial strains were computed. These computed values were then plotted to give friction and cohesion versus axial strain curves. Figure 11 shows CFS test set up.

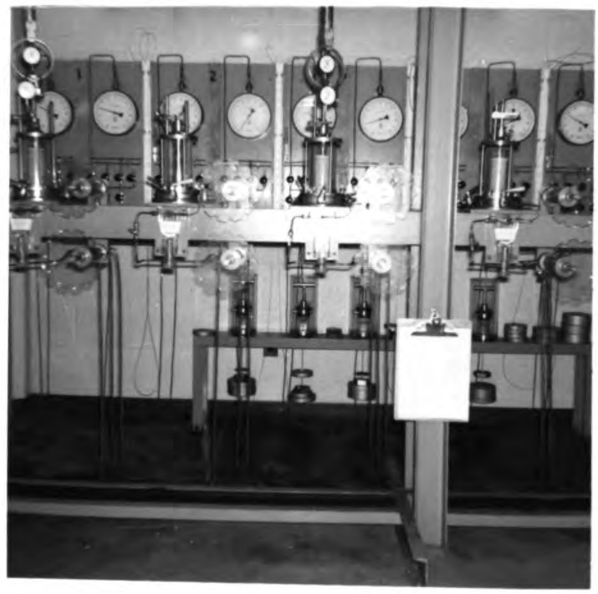

Figure 11 - CFS Test

Measurements recorded during the test were ($\sigma_1 - \sigma_3$), axial strain, and elapsed time. Early in the test these measurements were recorded after each 0.001 inch of axial deformation and later at increments of 0.1 percent axial strain. The proving ring was read continuously during the test and ($\sigma_1 - \sigma_3$) calculated. Corrections for change in area due to axial strain were made continuously. Each calculated value of ($\sigma_1 - \sigma_3$) was matched by the pore pressure. The equation used to calculate ($\sigma_1 - \sigma_3$) was

$$(\sigma_1 - \sigma_3) = \frac{\text{Proving ring dial reading x Proving ring constant}}{\text{Area at end of consolidation}}\left(1 - \frac{\text{Axial}}{\text{Strain}}\right)$$

(3.3-1)

c) Creep-CFS Test

The Creep-CFS test was a two-phase test performed on a single sample. The first phase was a Creep test as described above. After a certain time interval the CFS test was begun.

The pore pressure recorded at the end of the creep phase was used as the initial pore pressure for the CFS test and the load from the dead weight system was left in place. The difference in principal stresses calculated from the proving ring readings was added to the creep load to obtain the total difference in principal stresses ($\sigma_1 - \sigma_3$). To simplify recording of data during the test, the difference in principal stresses calculated from proving ring readings was matched by the total pore pressure less the initial value of pore pressure at the beginning of the CFS phase. Figure 12 shows Creep-CFS test.

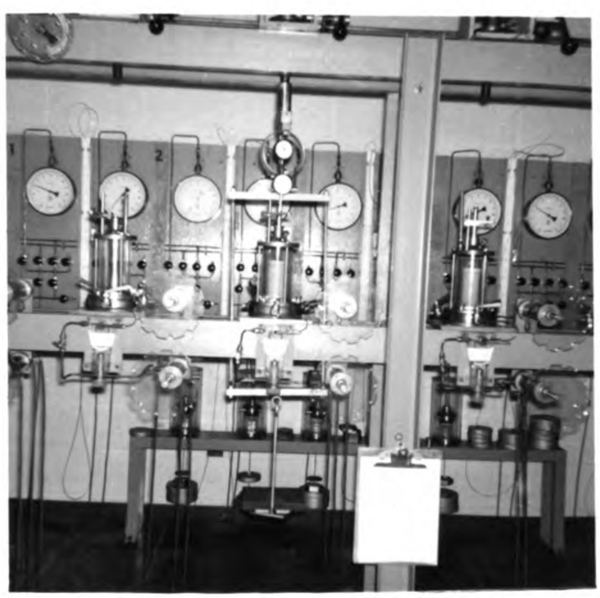

Figure 12 - Creep-CFS Test

3.4 Determination of τ_ϕ and τ_c from Creep Test

Inspection of equation (2.3-3) shows that a negligible or zero strain rate ($\frac{d\gamma}{dt}$) and a constant maximum shearing stress (τ) would allow the calculation of G as:

$$G = \tau/\gamma_F \qquad (3.4\text{-}1)$$

Where

τ = 0.5 x difference between principal stresses due to dead weight,

γ_F= Shear strain at time of negligible strain rate.

With this value of G it was possible to solve equation (2.3-1) for τ_ϕ at various strains. τ_c was now calculated from equation (2.3-3) knowing τ_ϕ and τ. Equation (2.3-3) could also be solved for ζ but ζ was not necessary to determine the stress transfer curves. Figure 14 and Figure 15 show typical creep curves used to calculate τ_ϕ and τ_c by Kelvin model analogy.

3.5 Determination of τ_ϕ and c' from Creep-CFS Test

To obtain the values for ϕ' and c' at the end of the creep phase of the Creep-CFS tests it was necessary to extrapolate the ϕ' versus axial strain and c' versus axial strain curves to the axial strain at end of creep. Since c' changes rapidly during the first stages of loading, the ϕ' versus axial strain curves were used for extrapolation. Data presented by Schmertmann (1960) show that the ϕ' versus axial strain curves for a particular saturated clay are similar while those of c' versus axial strain vary. Extrapolation of ϕ' is shown in Figures 16 and 17. From this the value of c' at the end of creep was calculated. Sample calculations for c' are given in the Appendix.

With known values of c' and ϕ' at the end of creep the values of τ_ϕ and τ_c were calculated from Mohr's circle as shown in Figure 13.

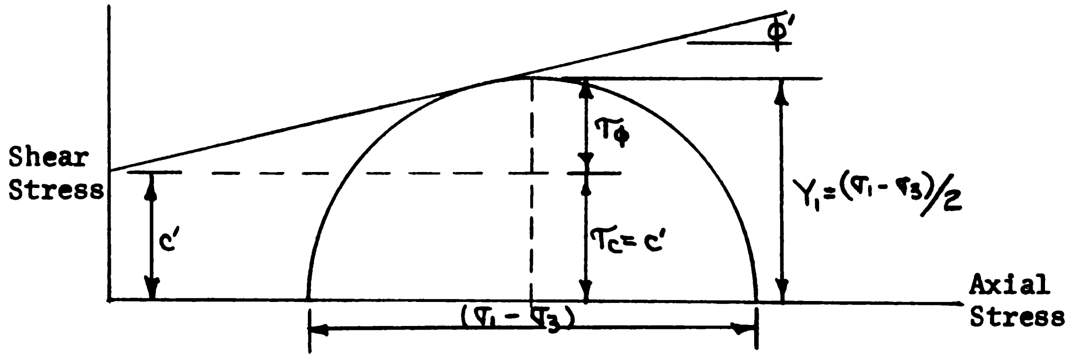

$(\sigma_1 - \sigma_3)$ = Principal stress difference due to dead load from creep phase

c' = Cohesion at end of creep

ϕ' = Friction at end of creep

$$\tau_c = c' \tag{3.5-1}$$

$$\tau_\phi = Y_1 - \tau_c \tag{3.5-2}$$

Figure 13 - Mohr's Circle

Calculations for τ_ϕ and τ_c are presented in the Appendix and Table 3 tabulates values of c' and τ_ϕ using the procedure described. A summary of triaxial tests is presented in Table 4 and typical data from all type tests run is presented in Appendix.

TABLE 3 - SUMMARY OF c' AND τ_ϕ VALUES

CREEP TESTS			CREEP-CFS TESTS		
Creep Time Min.	Cohesion End Creep Kg/cm^2	τ_ϕ End Creep Kg/cm^2	Creep Time Min.	Cohesion End Creep Kg/cm^2	τ_ϕ End Creep Kg/cm^2
COMPACTED CLAY					
60	0.407	0.093	120	0.469	0.031
125	.391	.109	480	.422	.078
460	.375	.125	960	.372	.128
825	.369	.131	1440	.376	.124
4320	.358	.142	4320	.356	.144
CONSOLIDATED CLAY					
30	0.485	0.090	60	0.564	0.011
125	.459	.115	240	.420	.155
250	.444	.131	1440	.393	.182
500	.428	.147	7200	.379	.196
7200	.401	.175			

TABLE 4 - SUMMARY OF TRIAXIAL TESTS

Test Desig.	Sample	Initial Water Content %	Final Water Content %	Consol. Pressure Kg/cm^2	Test Type	Avg. Strain Rate %/Hr.	Creep Load Kg/cm^2	Creep Time Hr.	Friction End Creep ϕ' Degrees	Cohesion End Creep c' Kg/cm^2
				COMPACTED CLAY						
C-CFS-1	C 16	43.0	32.1	2.0	CFS	0.80				
C-C-7	C 7	41.2	32.2	2.0	Creep-		1.00	72		
C-C-CFS-5	C 18	42.1	32.4	2.0	Creep-CFS	0.86	0.75	0.25	0.0	0.375
C-C-CFS-3	C 14	42.4	32.1	2.0	Creep-CFS	0.69	0.75	2	0.0	0.375
C-C-CFS-4	C 13	42.4	32.6	2.0	Creep-CFS	1.00	0.75	12	1.0	0.356
C-C-CFS-6	C 4	42.4	30.9	2.0	Creep-CFS	0.73	0.75	24	0.0	0.375
C-C-CFS-1	C 9	42.0	32.4	2.0	Creep-CFS	0.82	0.75	48	0.0	0.375
C-C-CFS-8	C 1	42.3	31.4	2.0	Creep-CFS	0.85	1.00	2	1.0	0.469
C-C-CFS-9	C 3	41.8	31.1	2.0	Creep-CFS	0.90	1.00	8	2.85	0.422
C-C-CFS-10	C 21	42.6	31.5	2.0	Creep-CFS	0.80	1.00	16	5.0	0.372
C-C-CFS-11	C 8	42.9	32.6	2.0	Creep-CFS	0.80	1.00	24	6.0	0.376
C-C-CFS-7	C 7	41.2	32.2	2.0	Creep-CFS	0.90	1.00	72	7.4	0.356

TABLE 4 CONTINUED

Test Desig.	Sample	Initial Water Content %	Final Water Content %	Consol. Pressure Kg/cm^2	Test Type	Avg. Strain Rate %/Hr.	Creep Load Kg/cm^2	Creep Time Hr.	Friction End Creep ϕ' Degrees	Cohesion End Creep c' Kg/cm^2
CONSOLIDATED CLAY										
F-CFS-1	F 5	49.8	32.5	2.0	CFS	1.20				
F-C-1	F 1	50.9	33.7	2.0	Creep		1.15	120		
F-C-CFS-4	F 4	48.9	32.4	2.0	Creep-CFS	1.10	1.15	1	0.4	0.564
F-C-CFS-2	F 2	47.9	32.6	2.0	Creep-CFS	1.10	1.15	4	6.2	0.420
F-C-CFS-3	F 3	51.9	33.1	2.0	Creep-CFS	0.85	1.15	24	9.0	0.393
F-C-CFS-1	F 1	50.9	33.7	2.0	Creep-CFS	0.85	1.15	120	12.2	0.379

TABLE 5 - TRIAXIAL TEST RESULTS AT END OF TESTS

Test Desig.	Strain	Upper Curve			Lower Curve				
	%	$(\sigma_1 - \sigma_3)$ Kg/cm^2	$\bar{\sigma}_1$ Kg/cm^2	$\bar{\sigma}_3$ Kg/cm^2	$(\sigma_1 - \sigma_3)$ Kg/cm^2	$\bar{\sigma}_1$ Kg/cm^2	$\bar{\sigma}_3$ Kg/cm^2	c' Kg/cm^2	ϕ' Deg.
C-CFS-1	8.0	1.42	2.00	0.58	1.36	1.75	0.39	0.538	7.8
C-C-CFS-5	6.0	1.41	2.38	.97	1.33	1.88	.55	.563	5.0
C-C-CFS-3	6.0	1.42	2.20	.78	1.32	1.70	.38	.537	6.8
C-C-CFS-4	6.0	1.34	2.05	.71	1.21	1.55	.34	.475	8.3
C-C-CFS-6	6.0	1.60	2.49	.89	1.47	1.99	.52	.546	9.0
C-C-CFS-1	3.0	1.17	1.75	.58	1.11	1.50	.39	.430	7.8
C-C-CFS-8	6.0	1.69	2.72	1.03	1.56	2.22	.66	.561	8.9
C-C-CFS-9	7.0	1.67	2.59	.92	1.55	2.09	.54	.600	7.5
C-C-CFS-10	6.0	1.57	2.48	.91	1.44	1.98	.54	.534	8.9
C-C-CFS-11	6.0	1.44	2.20	.76	1.33	1.70	.37	.541	7.1
C-C-CFS-7	7.0	1.42	2.14	.72	1.29	1.64	.35	.500	8.6
F-CFS-1	9.0	1.71	2.50	.79	1.51	2.00	.49	.459	14.6
F-C-CFS-4	9.0	1.71	2.63	.92	1.53	2.13	.60	.470	12.9
F-C-CFS-2	8.0	1.65	2.55	.90	1.48	2.05	.57	.476	12.5
F-C-CFS-3	6.0	1.51	2.27	.76	1.31	1.77	.46	.386	15.0
F-C-CFS-1	9.0	1.41	2.04	.63	1.23	1.54	.31	.433	12.0

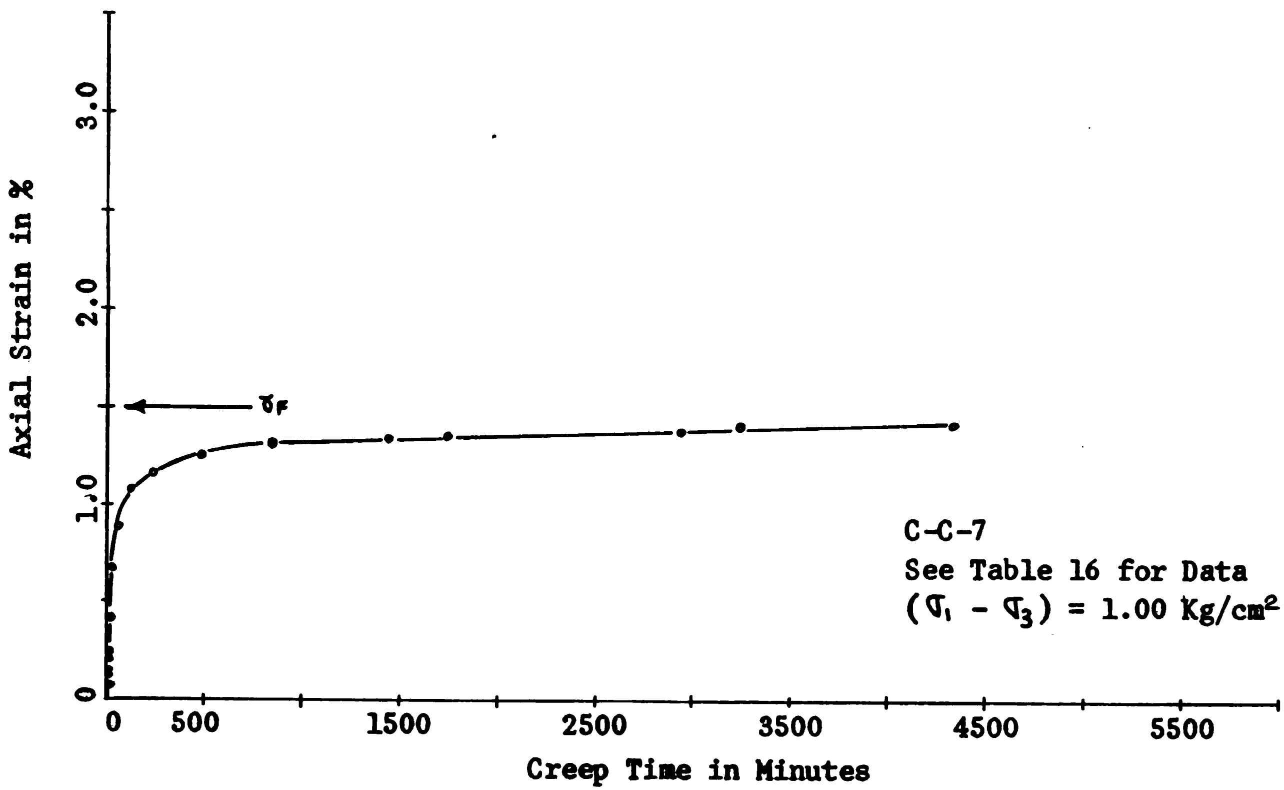

FIGURE 14 - CREEP CURVE FOR COMPACTED CLAY

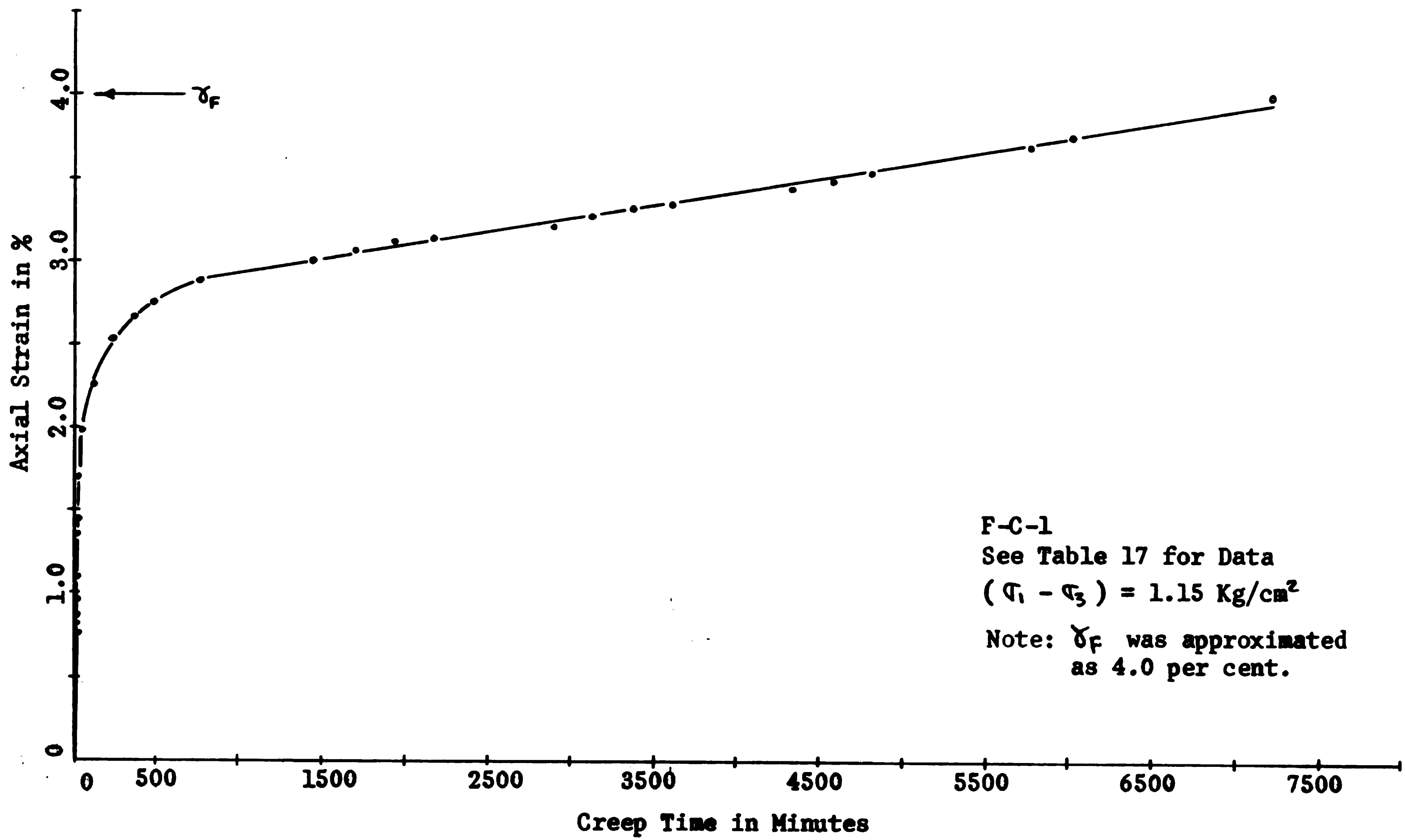

FIGURE 15 - CREEP CURVE FOR CONSOLIDATED CLAY

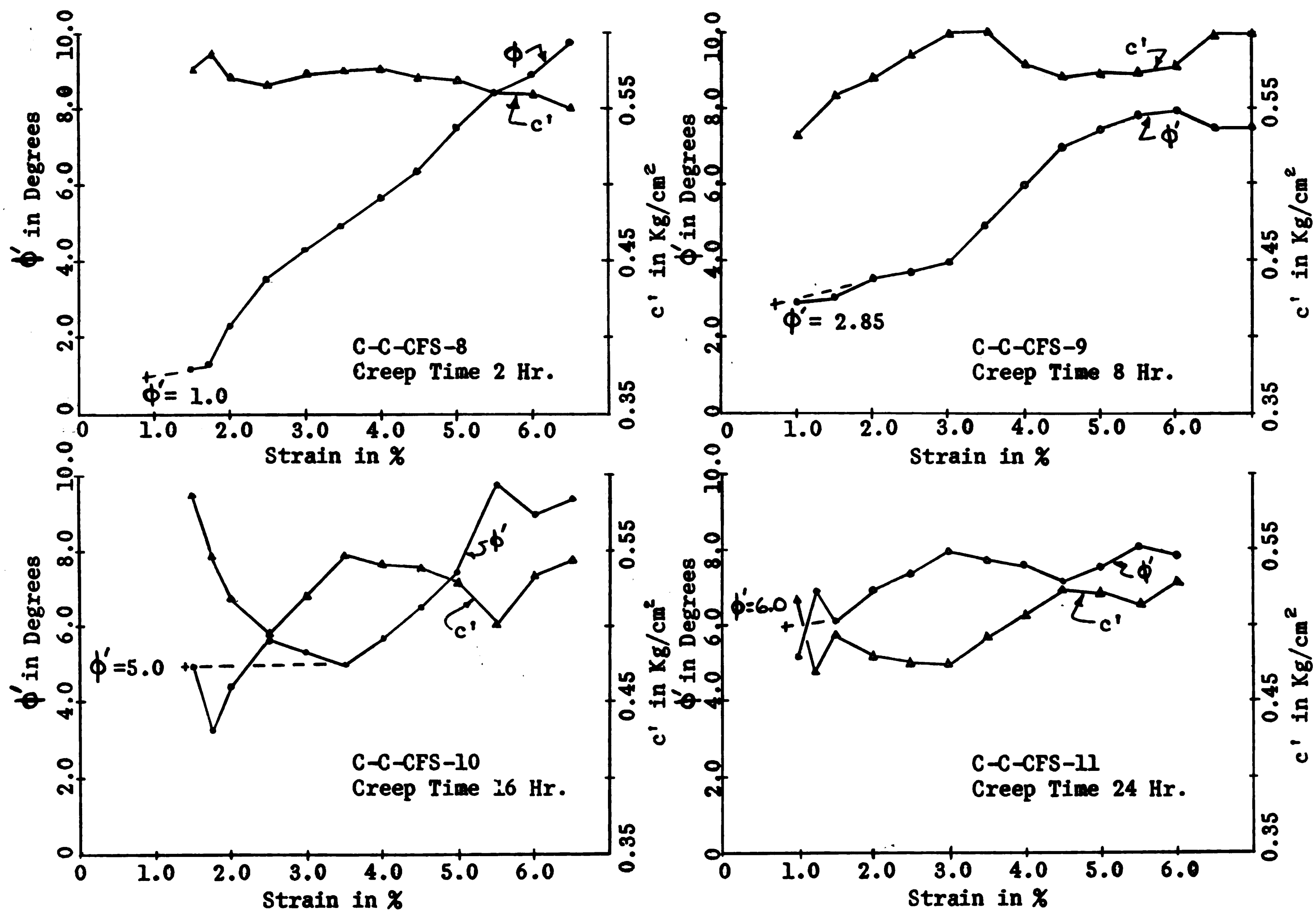

FIGURE 16 - EXTRAPOLATION OF φ' FOR COMPACTED CLAY

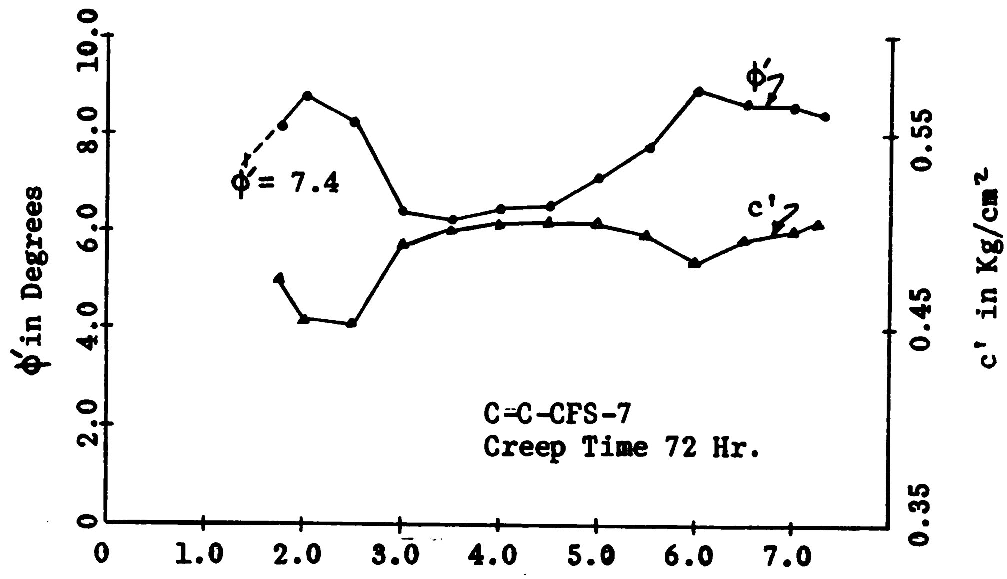

FIGURE 16 CONTINUED

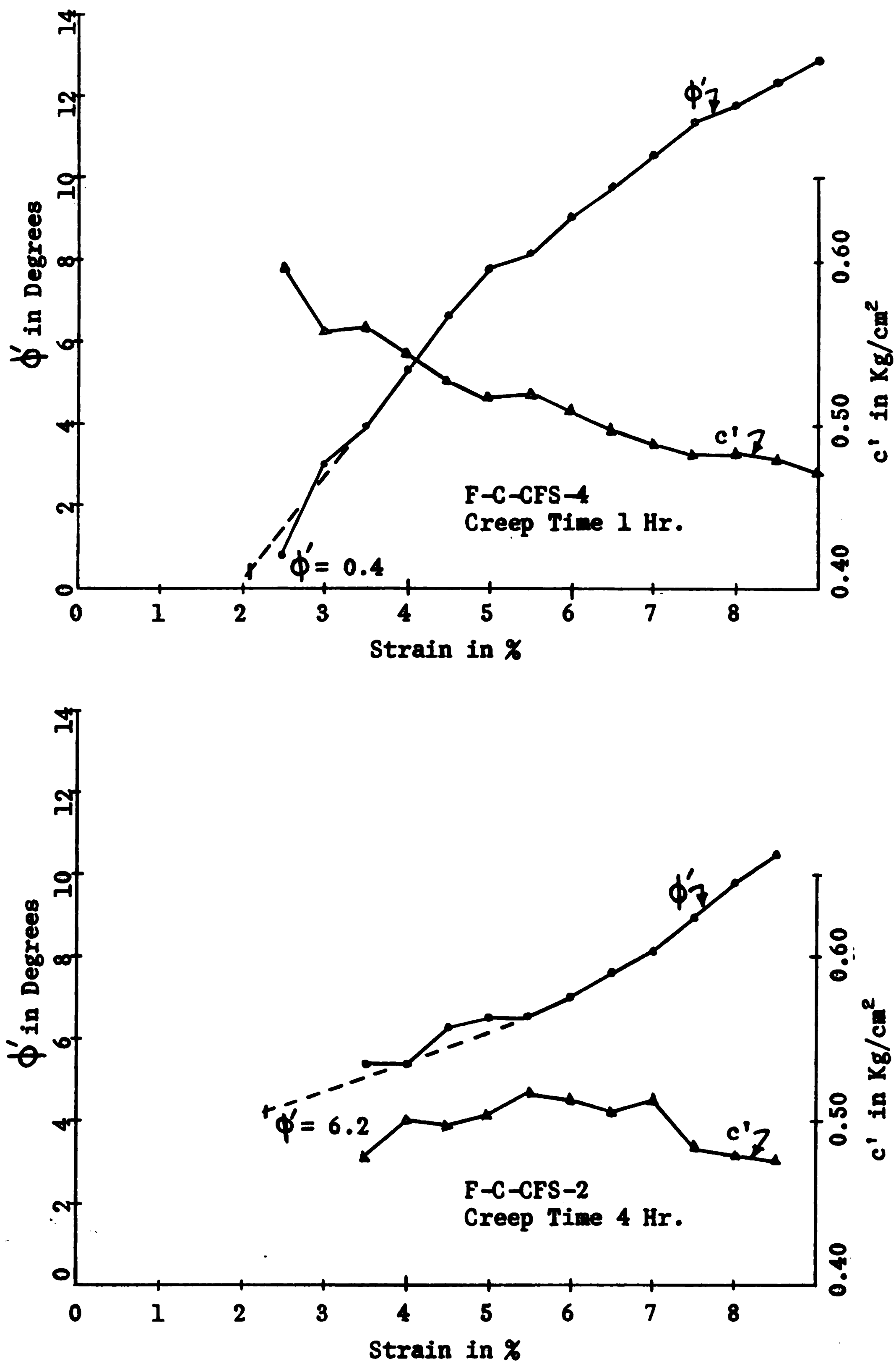

FIGURE 17 - EXTRAPOLATION OF ϕ' FOR CONSOLIDATED CLAY

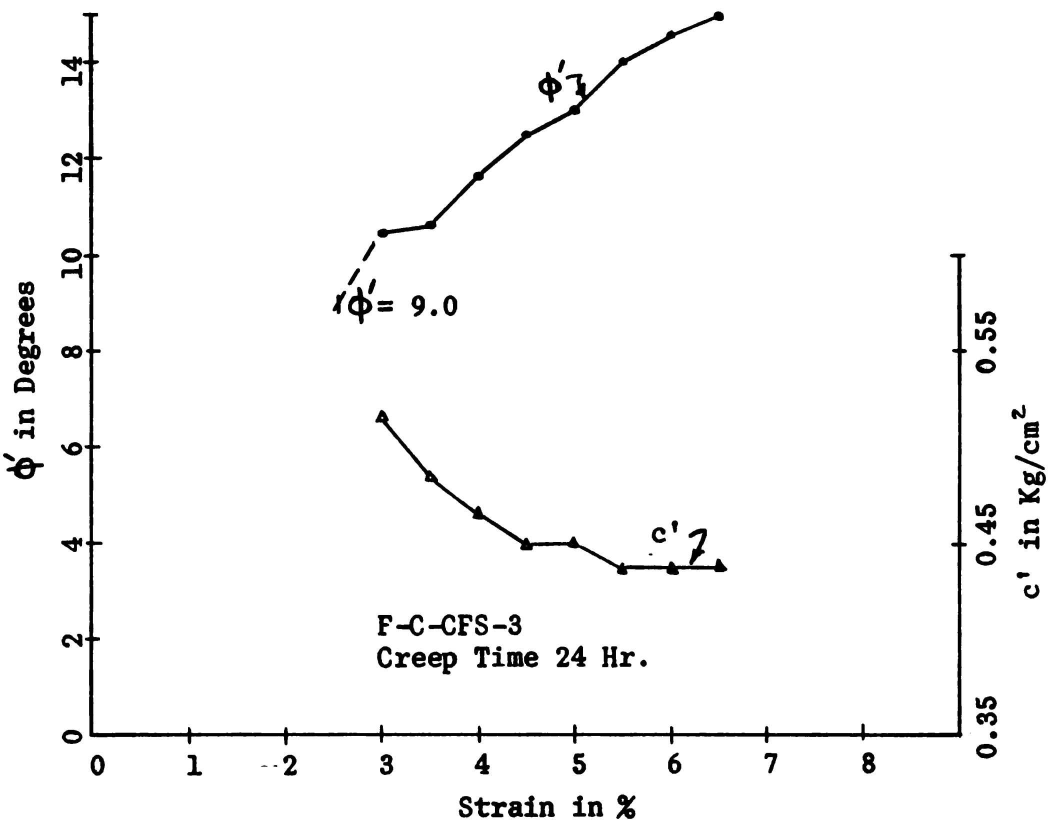

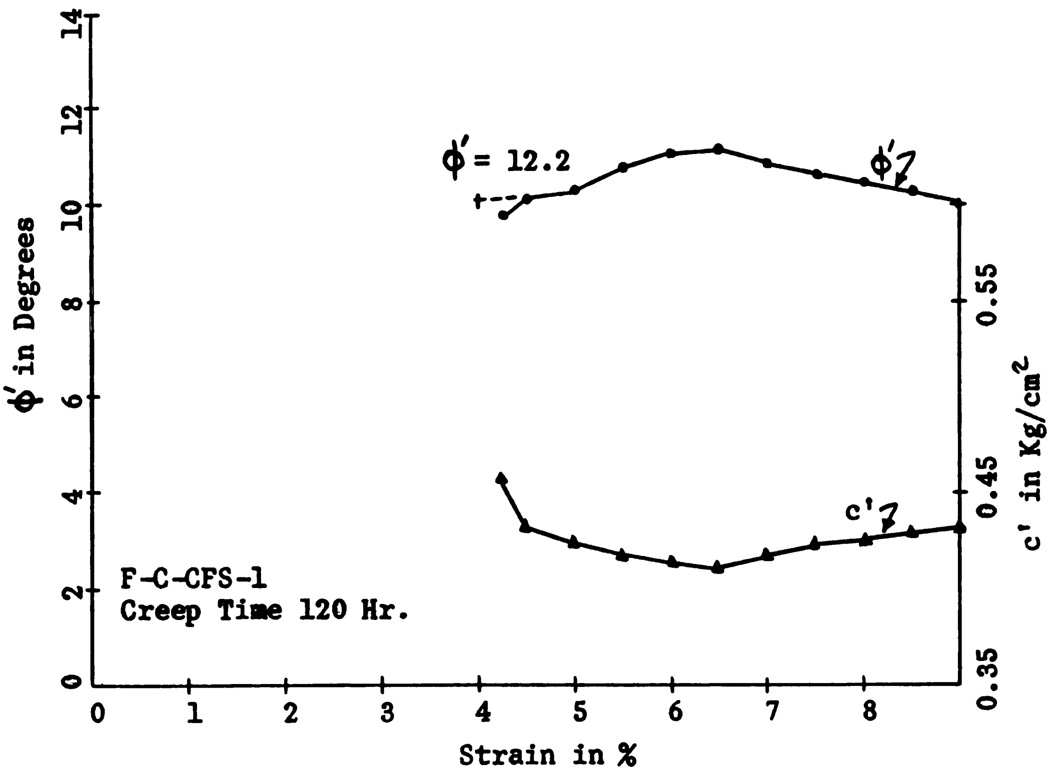

FIGURE 17 CONTINUED

IV RESULTS

Table 4 summarizes the results for the Creep-CFS tests under a creep load of 0.75 kilogram per square centimeter. (Specimens numbered C-C-CFS-1 and C-C-CFS-3 to 6). The friction angle at the end of all the creep periods was zero or nearly zero. This indicated that the entire creep load was resisted by the cohesive component of resistance with no stress transfer to the frictional component. A typical stress-strain curve for such a Creep-CFS test is shown in Figure 21. A curve of friction and cohesion versus axial strain is also plotted in Figure 21. These curves clearly show a value of zero for friction at the end of creep. From the results of the CFS test (Figure 22) it was noted at (σ_1 - σ_3) equal to 0.75 kilogram per square centimeter the two stress-strain curves are coincident, indicating a cohesive resistance only. Frictional resistance exists only if the two curves with different ($\bar{\sigma}_1$)s yield different strengths. Hence, a larger creep load was tried. It was decided to choose a creep load larger than the ($\sigma_1 - \sigma_3$) value at which the two stress-strain curves in a CFS test separate. Examination of Figure 22 and Figure 23 led to the choice of a creep load of 1.00 kilogram per square centimeter for the compacted specimens and 1.15 kilograms per square centimeter for the consolidated specimens.

Examination of the values of c' and ϕ' from the Creep-CFS tests in Table 4 indicates ϕ' for the compacted clay increased from 1.0 degree to 7.4 degrees with increasing time of creep. (Specimen numbers C-C-CFS-7 to 11) However, c' did not drop to zero but dropped to a shear stress of 0.35 kilogram per square centimeter. This was slightly below the shear stress at which the two stress-strain curves in Figure 22 started to separate. The value of ϕ' for the consolidated clay increased from 0.4 degree to 12.4 degrees with increasing time of creep. As before, c' did not drop to zero but to a shear stress of 0.37 kilogram per square centimeter. This shear stress was slightly below the shear stress at which the two stress-strain curves in Figure 23 separated.

It was evident from this observation that the Kelvin model described creep only after the creep load exceeded some constant value of cohesive resistance. The writer has called this value of cohesive resistance the threshold shear stress and denoted it as τ_T. τ_T was taken as 0.35 kilogram per square centimeter for the compacted clay and 0.37 kilogram per square centimeter for the consolidated clay. The threshold values are shown in Figure 18 and Figure 19. Calculations for τ_ϕ and c' are presented in the Appendix.

Figure 18 and Figure 19 show stress transfer curves for the compacted clay and the consolidated clay. The two curves in each figure are the stress transfer curves calculated from the creep curves shown in Figures 14 and 15 and measured from the Creep-CFS tests. If the friction and cohesion actually behaved as the viscous and elastic elements of the Kelvin rheological model the two curves should be the same.

The shear stress transfer from a viscous or cohesive resistance to an elastic or frictional resistance is clearly shown. Both types of clay exhibited a stress transfer behavior similar to that of the Kelvin model above the threshold shear stress τ_T . The numerical values computed for the two types of specimen used agree only approximately. For the compacted clay (Figure 18) the agreement is poor at short-time intervals (less than 700 minutes). In this time range values of ϕ' measured from the Creep-CFS tests are lower than those computed from the Creep test. Conversely, the values of c' are higher. For the consolidated clay (Figure 19) the agreement is poor at long-time intervals (longer than 1500 minutes). In this time range values of ϕ' measured from the Creep-CFS tests are also lower than those computed from the Creep test. Conversely, the values of c' are also higher. In spite of these differences the shape of the stress transfer curves measured from the Creep-CFS tests and computed from the Creep tests are similar.

The choice of τ_T affects the values computed from the Creep tests. Since this value is chosen somewhat arbitrarily it could account for the differences. Another possible explanation for the differences could be variation of G as creep progresses.

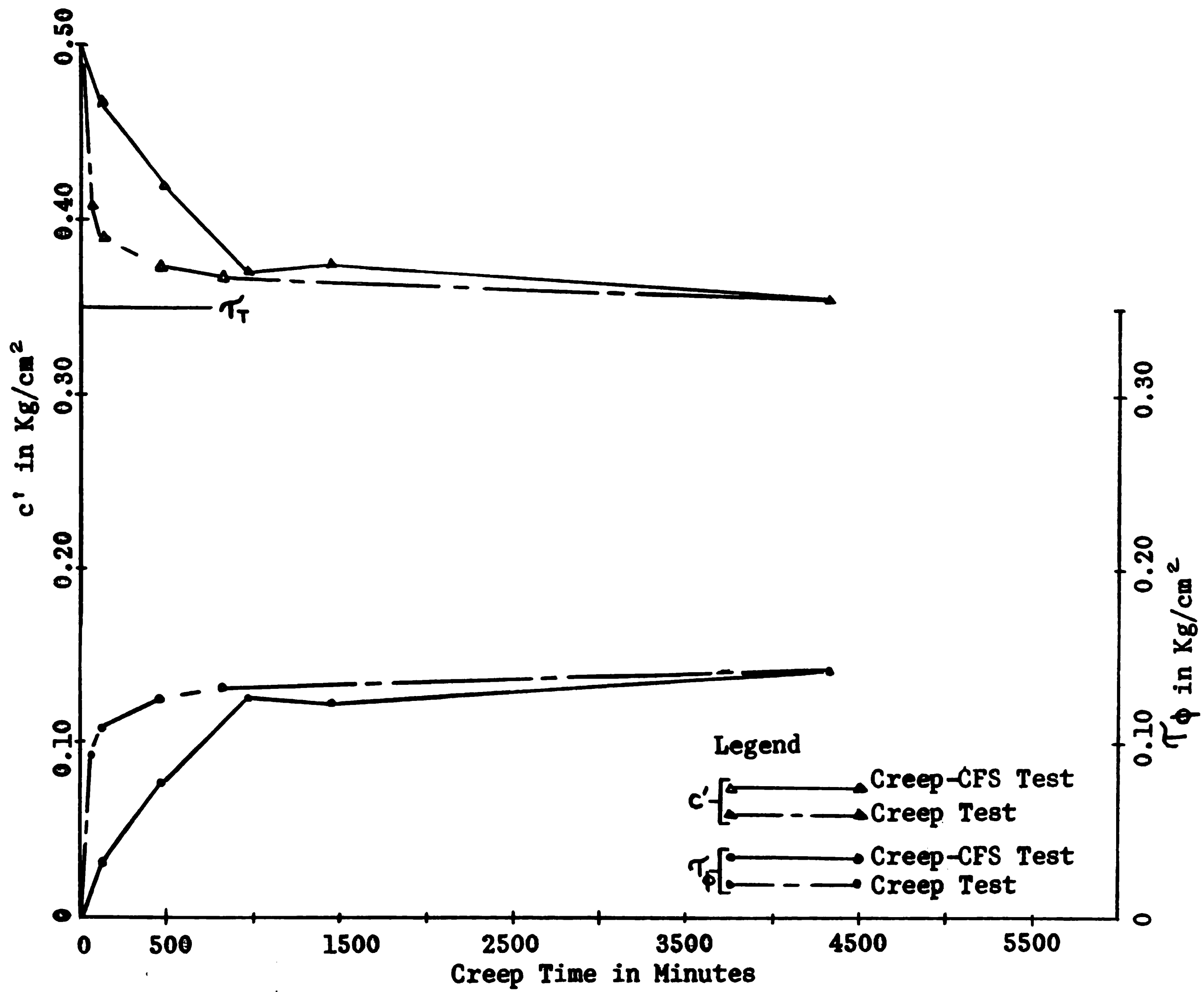

FIGURE 18 - STRESS TRANSFER FOR COMPACTED CLAY

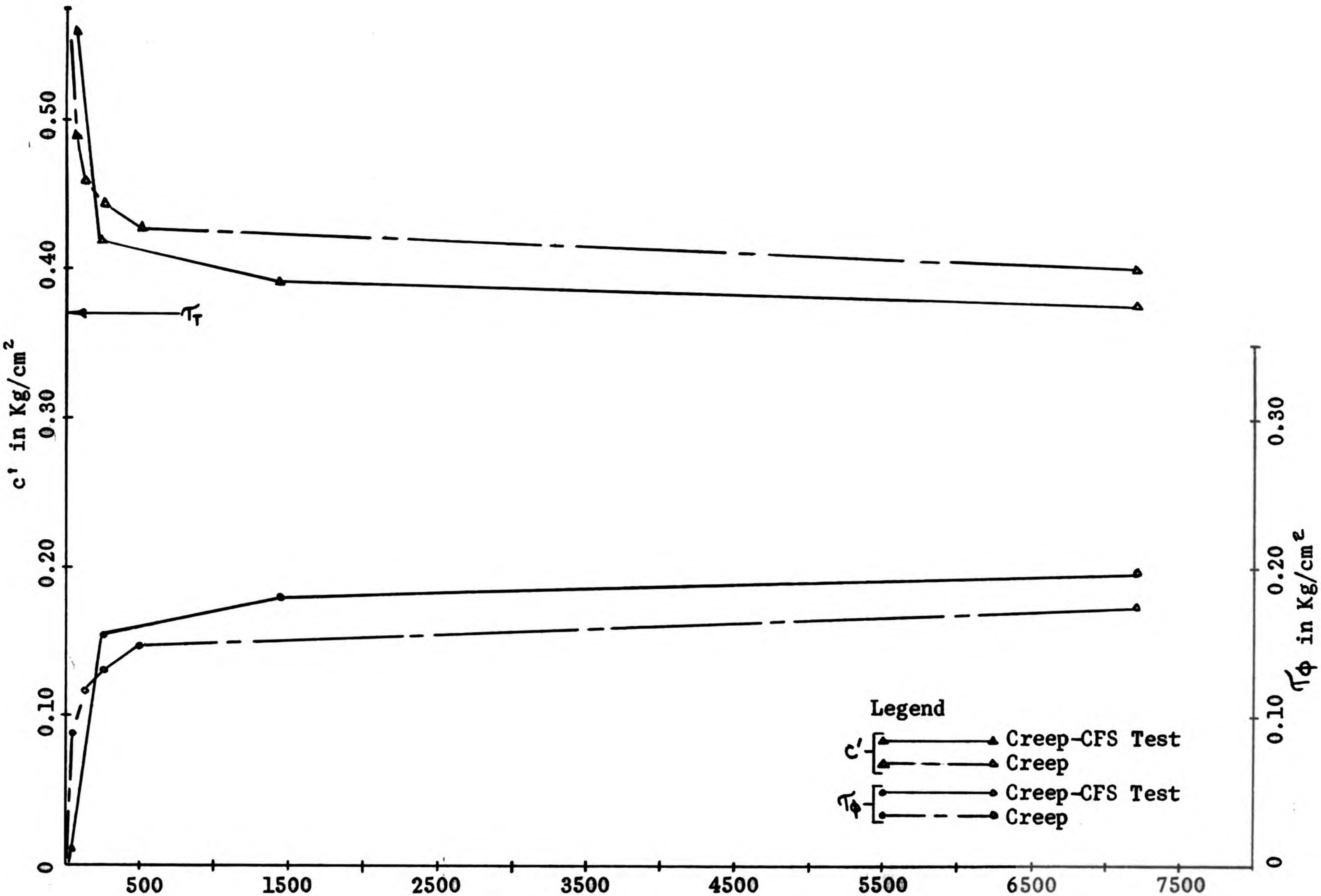

FIGURE 19 - STRESS TRANSFER FOR CONSOLIDATED CLAY

V CONCLUSIONS

5.1 Validity of Kelvin Model

The conclusions drawn here apply to the two types of clays tested.

1. Creep in a saturated clay may be represented approximately by the Kelvin model.
2. The clay behavior is such that stress is transferred from the component of cohesive resistance to the component of frictional resistance. This takes place only when the creep load exceeds a threshold shear stress.
3. The component of frictional resistance increases from zero and approaches its ultimate value after long-creep times. The component of cohesive resistance drops to the threshold shear stress after long-creep times.

5.2 Suggestions for Future Study

1. Clays of different mineral contents should be tested as described in this thesis to establish the general usefulness of the procedure.
2. A study should be made to find a simple rheologic model that will describe creep in a saturated clay to a closer approximation than the Kelvin model.
3. The threshold shear stress should be investigated.

VI BIBLIOGRAPHY

Bea, R. G. "Discussion of Friction and Cohesion of Saturated Clays," pp. 268-77. Journal of the Soil Mechanics and Foundations Division, vol. 89, SM 1. Ann Arbor: American Society of Engineers, 1963.

Bishop, Alan W., and D. J. Henkel. The Triaxial Test. Second Edition. London: Edward Arnold Ltd., 1962.

Buisman, A. S. Keverling. "Results of Long Duration Settlement Tests," pp. 103-06. Proceedings of the International Conference on Soil Mechanics and Foundation Engineering, vol. 1. Cambridge: 1936.

Casagrande, A. and S. D. Wilson. "Effect of Rate of Loading on the Strength of Clays and Shales at Constant Water Content," p. 251 Geotechnique, vol. 2. 1950.

Dillon, Howard B. "Structure and Identification of Clay Soils." Unpublished laboratory report, Soil Science 945, Michigan State University, East Lansing, 1963.

Geuze, E.C.W.A. "Compression, an Important Factor in the Shearing Test," pp. 141-42. Proceedings of the Second International Conference on Soil Mechanics and Foundation Engineering, vol. 3. Rotterdam: 1948.

Geuze, E.C.W.A. Introduction by General Reporter for Session 2, pp. 119-21. Proceedings of the Third International Conference on Soil Mechanics and Foundation Engineering, vol. 3. Switzerland: 1953.

Geuze, E.C.W.A. and T. K. Tan. "The Mechanical Behavior of Clays," Rheology, Ed. V. G. W. Harrison. New York: Academic Press Inc., 1954.

Haefeli, R. "Creep Problems in Soils, Snow and Ice," pp. 238-50. Proceedings of the Third International Conference on Soil Mechanics and Foundation Engineering, vol. 3. Switzerland: 1953.

Murayama, S. and T. Shibata. "Rheological Properties of Clays," pp. 269-73. Proceedings of the Fifth International Conference on Soil Mechanics and Foundation Engineering, vol. 1. Paris: 1961.

Rowe, P. W. "Ce=0 Hypothesis for Normally Loaded Clays at Equilibrium," pp. 189-92. Proceedings of the Fourth International Conference on Soil Mechanics and Foundation Engineering, vol. 1. London: 1957.

Schiffman, R. L. "The Use of Visco-Elastic Stress-Strain Laws in Soil Testing," pp. 131-55. ASTM Special Technical Publication No. 254. Philadelphia: American Society for Testing Materials, 1959.

Schmertmann, John H. and Jorj O. Osterberg. "An Experimental Study of the Development of Cohesion and Friction with Axial Strain in Saturated Cohesive Soils," pp. 643-94. Research Conference on Shear Strength of Cohesive Soils. Ann Arbor: American Society of Civil Engineers, 1960.

Terzaghi, Karl. Discussion of "Earth Pressure, Retaining Walls, Tunnels and Shafts in Soils," pp. 205-06. Proceedings of the Third International Conference on Soil Mechanics and Foundation Engineering, vol. 3. Switzerland: 1953.

Vialov, S. S. and A. M. Skibitsky. "Rheological Processes in Frozen Soils and Dense Clays," pp. 12-24. Proceedings of the Fourth International Conference on Soil Mechanics and Foundation Engineering, vol. 1. London: 1957.

Vialov, S. S. and A. M. Skibitsky. "Problems of the Rheology of Soils," pp. 387-91. Proceedings of the Fifth International Conference on Soil Mechanics and Foundation Engineering, vol. 1. Paris: 1961.

Wu, T. H., A. G. Douglas, and R. D. Goughnour. "Friction and Cohesion of Saturated Clays," pp. 1-23. Journal of the Soil Mechanics and Foundations Division, vol. 88 SM 3. Ann Arbor: American Society of Civil Engineers, 1962.

VII APPENDIX

7.1 Derivation of Data Table for CFS Test

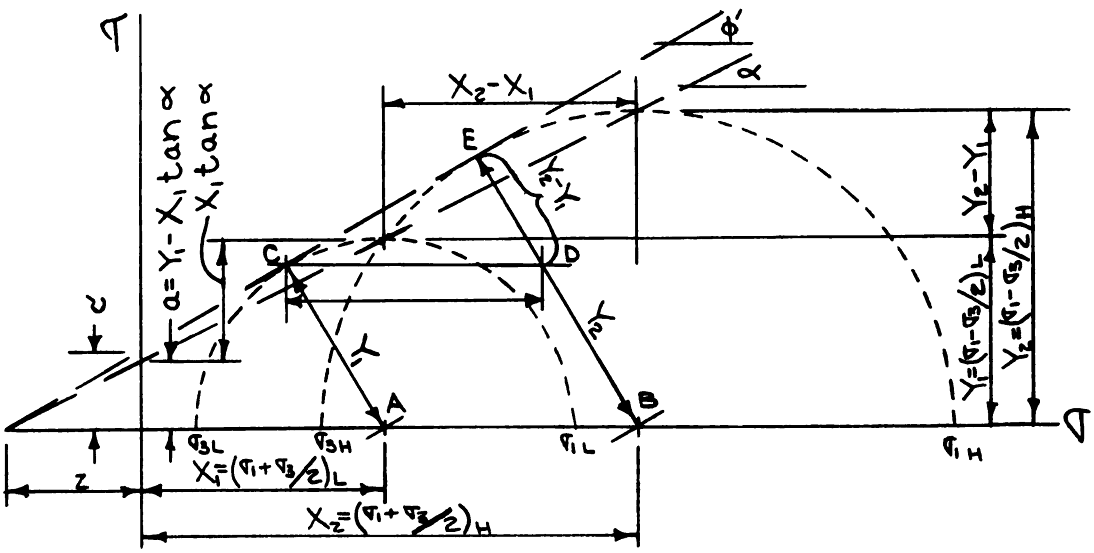

FIGURE 20 - MOHR'S CIRCLE FOR CFS TEST DATA TABLE

AB=CD and AC=BD

$\tan \alpha = (Y_2 - Y_1)/(X_2 - X_1)$

$\sin \phi' = (Y_2 - Y_1)/(X_2 - X_1)$

$\tan \alpha = \sin \phi'$

$\phi' = \sin^{-1}(Y_2 - Y_1)/(X_2 - X_1)$

$z = c'/\tan \phi'$ and $z = a/\tan \alpha$

$a = c' \cos \phi'$

$c' = a/\cos \phi'$

7.2 Typical Data for Tests Run (See following tables and figures)

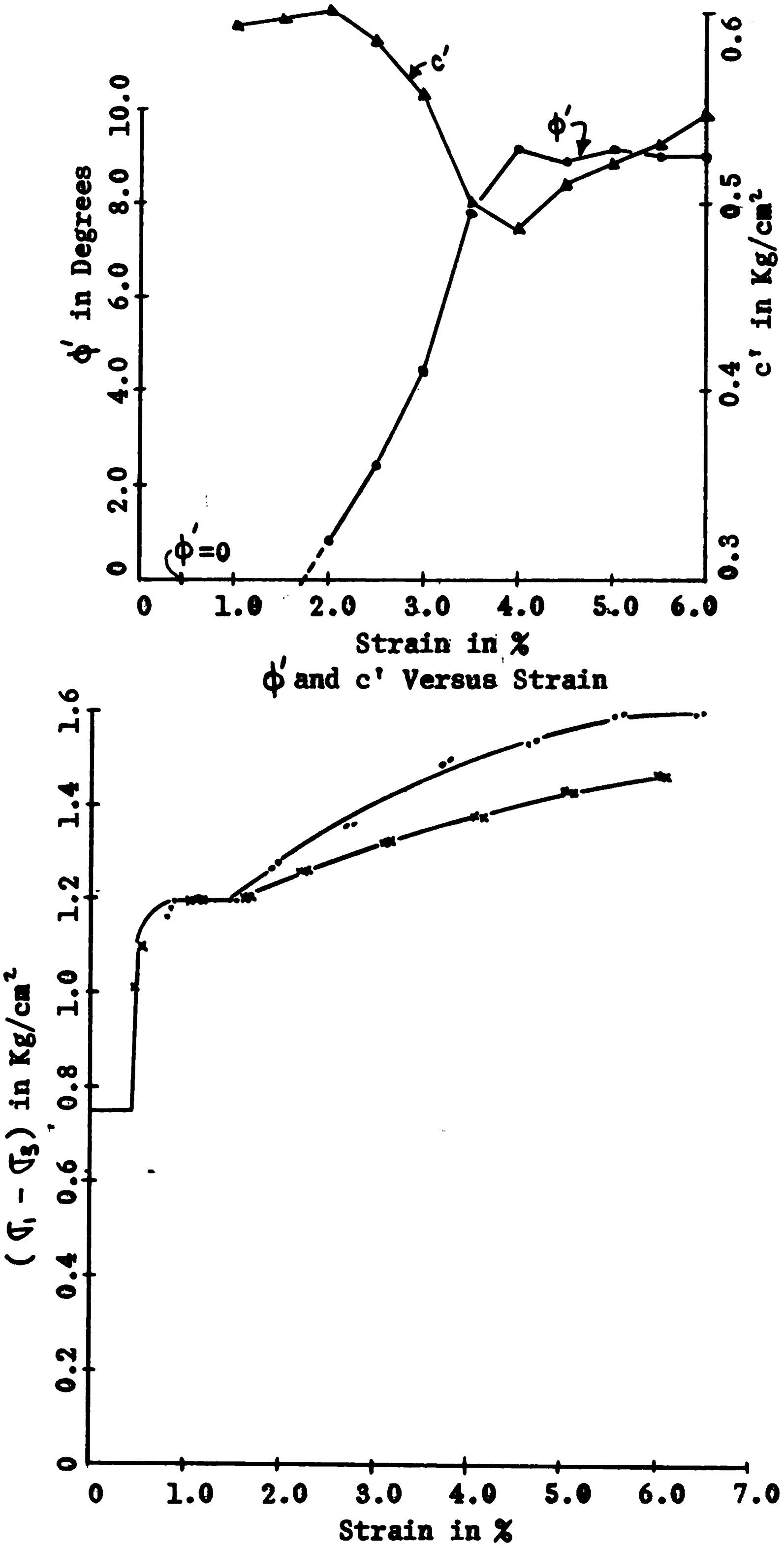

FIGURE 21 - TYPICAL STRESS-STRAIN CURVE FOR COMPACTED CLAY CREEP-CFS TEST (C-C-CFS-6)

TABLE 6 - GENERAL DATA SHEET

Date 3/21/63
Operator Holliday
Sample C 16

Test C-CFS-1
Cell 4

TRIMMINGS

Container No. 41

Cont. Wt. 29.47 (grams)

Cont. Wt. & Wet Wt. 71.12

Cont. Wt. & Dry Wt. 59.27

Water Wt. 11.85

Dry Wt. 29.80

Water Content 39.8%

SPECIMEN

Length 3.00 in = 7.62 cm

Volume 76.2 cm^3

Area 10.0 cm^2

	Initial	Final
Wt. of Spec.	137.73	127.10
Dry Wt. of Spec.	96.28	96.28
Wt. of Water	41.45	30.82
Water Content	43.0%	32.1%

TABLE 7 - CONSOLIDATION DATA SHEET

Cell 4
$\Delta V = 10.0\ cm^3$
$L = L_o(V/V_o) = 2.82$ in
Chamber Pressure 2.00 Kg/cm^2

Test C-CFS-1
$V = V_o - \Delta V = 66.2\ cm^3$
$A = A_o(V/V_o) = 9.11\ cm^2$
Back Pressure 1.5 Kg/cm^2

Date	Time	Elapsed Time Min.	Burette cc	Drainage cc
3/21/63	1606	0.0	0.0	0.0
		0.25	1.5	1.5
		0.50	1.8	1.8
		1.00	2.0	2.0
		2.00	2.4	2.4
		5.0	3.2	3.2
		10.0	4.2	4.2
		23.0	6.2	6.2
		30.0	6.9---0.0	6.9
		60.0	2.4	9.3
		136.0	4.8---0.0	11.7
	2108	302.0	1.2	12.9
3/22/63	0842	996.0	1.2	12.9
	1502	1356.0	1.3	13.0
	1621	1455.0	1.3	13.0
	1634	Back Pressure Applied		

TABLE 8 - CFS DATA SHEET

Cell 4
Chamber Pressure 3.5 Kg/cm^2
Proving Ring Number 684
Proving Ring Constant 0.1470 Kg/div.

Test C-CFS-1
Date 3/25/63
* ½Kg Wt. Added
** ½Kg Wt. Removed

$$(\sigma_1 - \sigma_3) = \frac{N(PRC)}{A}(1-\epsilon) = \frac{N(147)}{9.11}(1-\epsilon)$$

Time	Load Dial $N \times 10^{-4}$	Strain Dial in.	Strain %	$(\sigma_1 - \sigma_3)$ Kg/cm^2	$\Delta u = (\sigma_1 - \sigma_3)$ Kg/cm^2	Constant Pressure Cell Kg/cm^2
0915	0.0600	0.0	0.0	0.0	0.0	1.5
0930	.0630	0.0028	0.1	0.484	0.484	1.5
0940	.0646	.0056	.2	.742	.742	1.5
0946	.0653	.0071	.25	.854	.854	* 1.75
0949	.0655	.0085	.30	.889	.889	1.75
0953	.0656	.0099	.35	.902	.902	1.75
1008	.0661	.0155	.55	.980	.980	** 1.50
1012	.0661	.0169	.60	.980	.980	1.50
1016	.0662	.0183	.65	.994	.994	* 1.75
1021	.0662	.0197	.70	.994	.994	1.75
1042	.0664	.0282	1.00	1.025	1.025	** 1.50
1050	.0664	.0310	1.1	1.03	1.03	1.50
1119	.0640	.0424	1.5	1.03	1.03	* 1.75
1125	.0650	.0451	1.6	1.035	1.035	1.75
1139	.0660	.0508	1.8	1.05	1.05	** 1.5
1148	.0669	.0536	1.9	1.09	1.09	1.5
1220	.0667	.0649	2.3	1.065	1.065	* 1.75
1228	.0667	.0676	2.4	1.055	1.055	1.75

TABLE 8 CONTINUED

Cell 4 Test C-CFS-1

Time	Load Dial $N \times 10^{-4}$	Strain Dial in.	Strain %	$(\sigma_1 - \sigma_3)$ Kg/cm²	$\Delta u = (\sigma_1 - \sigma_3)$ Kg/cm²	Constant Pressure Cell Kg/cm²
1300	.0673	.0790	2.8	1.14	1.14	** 1.50
1308	.0674	.0817	2.9	1.155	1.155	1.50
1321	.0673	.0874	3.1	1.14	1.14	* 1.75
1327	.0673	.0904	3.2	1.14	1.14	1.75
1343	.0677	.0959	3.4	1.20	1.20	** 1.50
1347	.0677	.0986	3.5	1.20	1.20	1.50
1413	.0676	.1071	3.8	1.18	1.18	* 1.75
1419	.0676	.1100	3.9	1.85	1.85	1.75
1445	.0681	.119	4.2	1.25	1.25	** 1.50
1451	.0682	.121	4.3	1.26	1.26	1.50
1508	.0680	.127	4.5	1.23	1.23	* 1.75
1515	.0679	.130	4.6	1.22	1.22	1.75
1537	.0684	.138	4.9	1.30	1.30	** 1.50
1544	.0685	.141	5.0	1.31	1.31	1.50
1600	.0683	.147	5.2	1.27	1.27	* 1.75
1608	.0683	.149	5.3	1.27	1.27	1.75
1634	.0688	.158	5.6	1.34	1.34	** 1.50
1637	.0689	.161	5.7	1.35	1.35	1.50
1741	.0689	.1861	6.6	1.35	1.35	* 1.75
1749	.0689	.1890	6.7	1.34	1.34	1.75
1805	.0692	.194	6.9	1.39	1.39	** 1.50

TABLE 8 CONTINUED

Cell 4 Test C-CFS-1

Time	Load Dial N x 10^{-4}	Strain Dial in	Strain %	$(\sigma_1 - \sigma_3)$ Kg/cm^2	$\Delta u = (\sigma_1 - \sigma_3)$ Kg/cm^2	Constant Pressure Cell Kg/cm^2
1812	.0692	.197	7.0	1.39	1.39	1.50
1824	.0690	.203	7.2	1.35	1.35	* 1.75
1830	.0690	.205	7.3	1.35	1.35	1.75
1846	.0693	.2110	7.5	1.39	1.39	** 1.5
1853	.0695	.2138	7.6	1.41	1.41	1.5
1908	.0692	.220	7.8	1.37	1.37	* 1.75
1916	.0691	.222	7.9	1.35	1.35	1.75
1930	.0695	.2285	8.1	1.41	1.41	** 1.50
1938	.0697	.231	8.2	1.42	1.42	1.50

TABLE 9 - CFS DATA SUMMARY

Upper Curve $\bar{\sigma}_1 = 2.00$ | Lower Curve $\bar{\sigma}_1 = 1.75$ | Test: C-CFS-1

Strain %	$(\sigma_1-\sigma_3)$	$\bar{\sigma}_3$	$\frac{1}{2}(\sigma_1-\sigma_3)$ Y_2	$\frac{1}{2}(\sigma_1+\sigma_3)$ X_2	$(\sigma_1-\sigma_3)$	$\bar{\sigma}_3$	$\frac{1}{2}(\sigma_1-\sigma_3)$ Y_1	$\frac{1}{2}(\sigma_1+\sigma_3)$ X_1	Y_2-Y_1	X_2-X_1	$\tan\alpha = \sin\phi'$	ϕ' Deg.	$X_1\tan\alpha$	$Y_1-X_1\tan\alpha = a = c'\cos\phi'$	c' Kg/cm^2
0.4	0.93	1.07	0.465	1.535	0.92	0.83	0.460	1.290	0.005	0.245	0.0204	1.17	0.0263	0.434	0.435
.5	.96	1.04	.480	1.520	.94	.81	.470	1.280	.010	.240	.0417	2.39	.0534	.417	.418
.75	1.00	1.00	.500	1.500	.98	.77	.490	1.260	.010	.240	.0417	2.39	.0526	.438	.439
1.0	1.03	.97	.515	1.485	1.01	.74	.505	1.245	.010	.240	.0417	2.39	.0520	.453	.454
1.5	1.06	.94	.530	1.470	1.03	.72	.515	1.235	.015	.235	.0640	3.67	.0790	.436	.437
2.0	1.10	.90	.550	1.450	1.06	.69	.530	1.220	.020	.230	.0870	4.99	.1061	.424	.426
2.5	1.13	.87	.565	1.435	1.09	.66	.545	1.205	.020	.230	.0870	4.99	.1049	.440	.442
3.0	1.16	.84	.580	1.420	1.12	.63	.560	1.190	.020	.230	.0870	4.99	.1035	.456	.458
3.5	1.20	.80	.600	1.400	1.15	.60	.575	1.175	.025	.225	.1110	6.36	.1302	.445	.448
4.0	1.24	.76	.620	1.380	1.18	.57	.590	1.160	.030	.220	.1361	7.84	.1580	.432	.436
4.5	1.28	.72	.640	1.360	1.22	.53	.610	1.140	.030	.220	.1361	7.84	.1550	.455	.459
5.0	1.31	.69	.655	1.345	1.25	.50	.625	1.125	.030	.220	.1361	7.84	.1534	.472	.476
5.5	1.34	.66	.670	1.330	1.28	.47	.640	1.110	.030	.220	.1361	7.84	.1510	.489	.493
6.0	1.37	.63	.685	1.315	1.31	.44	.655	1.095	.030	.220	.1361	7.84	.1495	.505	.509
6.5	1.39	.61	.695	1.305	1.33	.42	.665	1.085	.030	.220	.1361	7.84	.1475	.517	.521
7.0	1.40	.60	.700	1.300	1.34	.41	.670	1.080	.030	.220	.1361	7.84	.1470	.523	.527
8.0	1.42	.58	.710	1.290	1.36	.39	.680	1.070	.030	.220	.1361	7.84	.1455	.534	.538

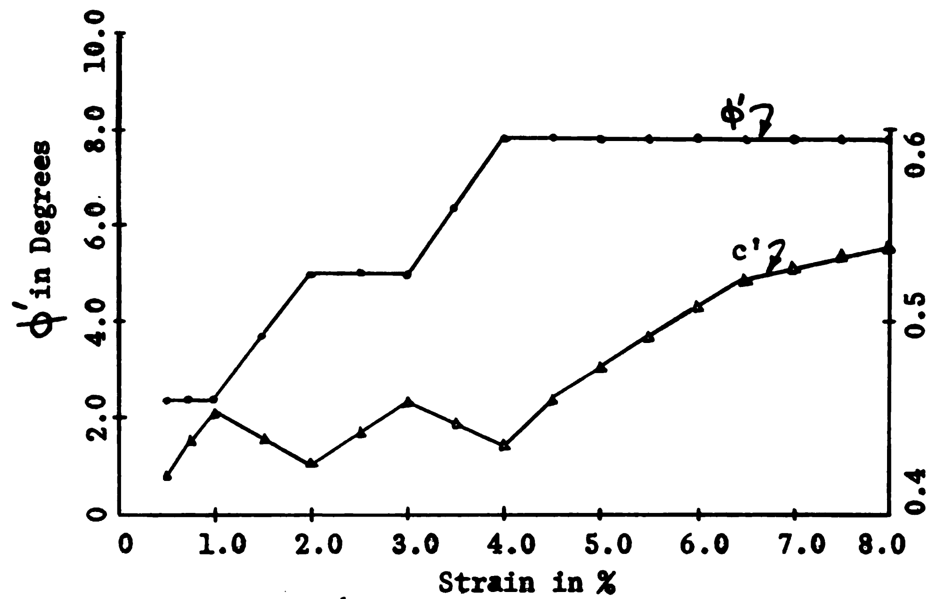

φ' and c' Versus Strain

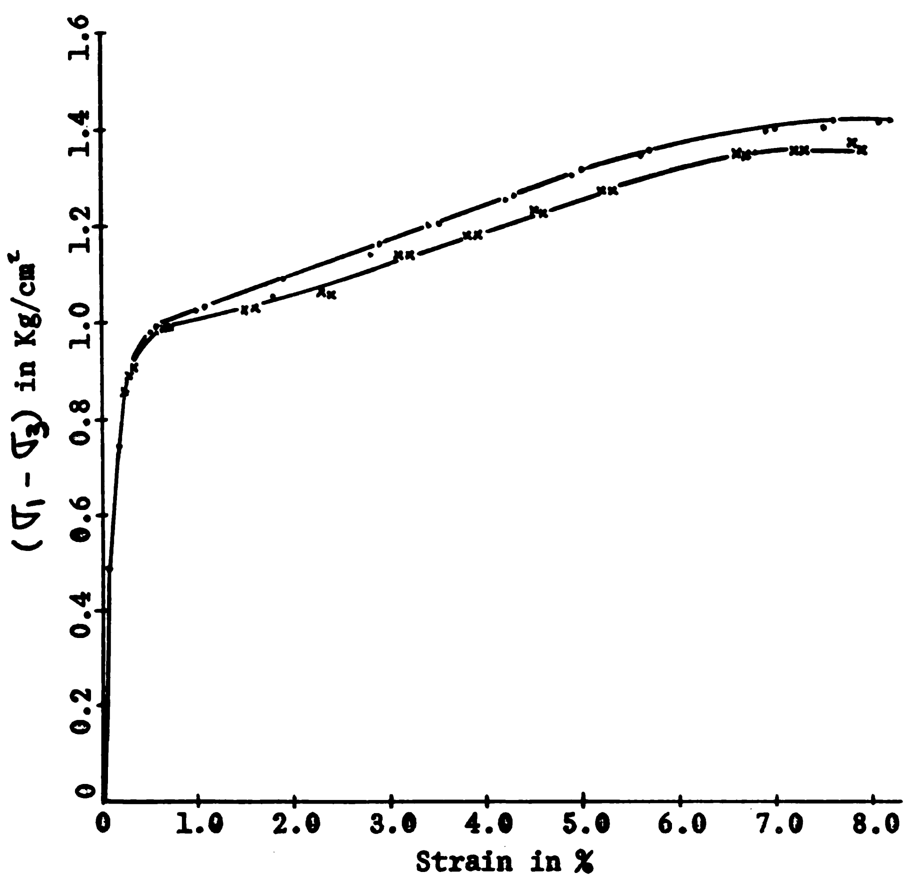

FIGURE 22 - STRESS-STRAIN CURVE FOR TEST C-CFS-1

TABLE 10 - GENERAL DATA SHEET

Date 6/18/63
Operator Holliday
Sample F 5

Test F-CFS-1
Cell 1

TRIMMINGS

Container No. 210

Cont. Wt. 20.61 (grams)

Cont. Wt. & Wet Wt. 63.86

Cont. Wt. & Dry Wt. 50.53

Water Wt. 13.33

Dry Wt. 29.92

Water Content 44.5%

SPECIMEN

Length 2.8 in = 7.11 cm

Volume 71.1 cm^3

Area 10.0 cm^2

	Initial	Final
Wt. of Spec.	129.06	114.12
Dry Wt. of Spec.	86.13	86.13
Wt. of Water	42.93	27.99
Water Content	49.8%	32.5%

TABLE 11 - CONSOLIDATION DATA SHEET

Cell 1
$\Delta V = 17.8\ cm^3$
$L = L_O(V/V_O) = 2.54$ in.
Chamber Pressure 2.00 Kg/cm^2

Test F-CFS-1
$V = V_O - \Delta V = 53.3\ cm^3$
$A = A_O(V/V_O) = 8.26\ cm^2$
Back Pressure 1.5 Kg/cm^2

Date	Time	Elapsed Time Min.	Burette cc	Drainage cc
6/18/63	1431	0.0	10.0	0.0
		.25	8.6	1.4
		.5	8.2	1.8
		1.0	7.6	2.4
		2.0	6.8	3.2
		5.0	5.2	4.8
		10.0	3.1	6.9
		15.0	1.7---10.0	8.3
		35.0	6.1	12.2
		60.0	3.5---10.0	14.8
	1631	120.0	7.8	17.0
	1715	164.0	7.2	17.6
	2131	420.0	6.5	18.3
6/19/63	1031	1200.0	6.1	18.7
	1431	1440.0	6.0	18.8
	1442	Back Pressure Applied		

TABLE 12 - CFS DATA SHEET

Cell 1
Chamber Pressure 3.5 Kg/cm^2
Proving Ring Number 3144
Proving Ring Constant 0.0455 Kg/div.

Test F-CFS-1
Date 6/20/63
*1 Kg Wt. Added
**1 Kg Wt. Removed

$$(\sigma_1 - \sigma_3) = \frac{N(PRC)}{A}(1-\epsilon) = \frac{N(.0455)}{8.26}(1-\epsilon)$$

Time	Load Dial N x 10^{-4}	Strain Dial in.	Strain %	$(\sigma_1 - \sigma_3)$ Kg/cm^2	$\Delta u = (\sigma_1 - \sigma_3)$ Kg/cm^2	Constant Pressure Cell Kg/cm^2
0826	0.0200	0.0	0.0	0.0	0.0	1.50
0849	.0290	.003	.1	.495	.495	1.50
0914	.0376	.005	.2	.970	.970	1.50
0951	.0422	.020	.8	1.215	1.215	** 1.00
0956	.0427	.023	.9	1.240	1.240	1.00
1011	.0429	.030	1.2	1.249	1.249	* 1.50
1016	.0431	.033	1.3	1.255	1.255	1.50
1058	.0461	.053	2.1	1.410	1.410	** 1.00
1104	.0465	.056	2.2	1.430	1.430	1.00
1125	.0454	.069	2.7	1.360	1.360	* 1.50
1128	.0455	.071	2.8	1.368	1.368	1.50
1223	.0494	.967	3.8	1.560	1.560	** 1.00
1227	.0496	.099	3.9	1.560	1.560	1.00
1244	.0473	.112	4.4	1.435	1.435	* 1.50
1250	.0474	.114	4.5	1.440	1.440	1.50
1335	.0510	.135	5.3	1.615	1.615	** 1.00
1340	.0512	.137	5.4	1.622	1.622	1.00
1358	.0485	.150	5.9	1.475	1.475	* 1.50

TABLE 12 CONTINUED

Cell 1 Test F-CFS-1

Time	Load Dial N x 10^{-4}	Strain Dial in.	Strain %	$(\sigma_1 - \sigma_3)$ Kg/cm^2	$\Delta u = (\sigma_1 - \sigma_3)$ Kg/cm^2	Constant Pressure Cell Kg/cm^2
1401	.0485	.152	6.0	1.475	1.475	1.50
1446	.0526	.173	6.8	1.671	1.671	** 1.00
1452	.0528	.175	6.9	1.685	1.685	1.00
1514	.0495	.190	7.5	1.505	1.505	* 1.50
1516	.0495	.193	7.6	1.505	1.505	1.50
1556	.0535	.211	8.3	1.690	1.690	** 1.00
1604	.0537	.214	8.4	1.701	1.701	1.00
1621	.0502	.229	9.0	1.510	1.510	* 1.50
1627	.0502	.231	9.1	1.510	1.510	1.50
1714	.0545	.252	9.9	1.710	1.710	** 1.00
1720	.0547	.254	10.0	1.713	1.713	1.00

TABLE 13 - CFS DATA SUMMARY

Upper Curve
$\bar{\sigma}_1 = 2.500$

Lower Curve
$\bar{\sigma}_1 = 2.000$

Test: F-CFS-1

Strain %	$(\sigma_1-\sigma_3)$	$\bar{\sigma}_3$	$\frac{1}{2}(\sigma_1-\sigma_3)$ Y_2	$\frac{1}{2}(\sigma_1+\sigma_3)$ X_2	$(\sigma_1-\sigma_3)$	$\bar{\sigma}_3$	$\frac{1}{2}(\sigma_1-\sigma_3)$ Y_1	$\frac{1}{2}(\sigma_1+\sigma_3)$ X_1	Y_2-Y_1	X_2-X_1	$\tan\alpha = \sin\phi'$	ϕ' Deg.	$X_1\tan\alpha$	$Y_1-X_1\tan\alpha = a = c'\cos\phi'$	c' Kg/cm
0.5	1.160	1.340	0.580	1.920	1.140	0.860	0.570	1.430	0.010	0.490	0.0204	1.16	0.0292	0.541	0.542
1.0	1.250	1.250	.625	1.875	1.210	.790	.605	1.395	.020	.480	.0417	2.38	.0582	.547	.548
1.5	1.330	1.170	.665	1.835	1.265	.735	.633	1.368	.032	.467	.0685	3.92	.0936	.540	.541
2.0	1.400	1.100	.700	1.800	1.315	.685	.657	1.342	.043	.458	.0940	5.38	.126	.531	.534
2.5	1.460	1.040	.730	1.770	1.350	.650	.675	1.325	.055	.445	.124	7.10	.164	.511	.516
3.0	1.505	.995	.753	1.748	1.375	.625	.687	1.312	.066	.436	.151	8.66	.198	.489	.494
3.5	1.543	.957	.771	1.728	1.395	.605	.697	1.302	.074	.426	.174	10.0	.224	.473	.481
4.0	1.570	.930	.785	1.715	1.420	.580	.710	1.290	.075	.425	.177	10.2	.229	.481	.489
4.5	1.590	.910	.795	1.705	1.440	.560	.720	1.280	.075	.425	.177	10.2	.227	.493	.500
5.0	1.608	.892	.804	1.696	1.450	.550	.725	1.275	.079	.421	.188	10.85	.240	.485	.494
5.5	1.625	.875	.813	1.688	1.465	.535	.733	1.268	.080	.420	.190	11.0	.241	.492	.501
6.0	1.640	.860	.820	1.680	1.480	.520	.740	1.260	.080	.420	.190	11.0	.239	.501	.510
6.5	1.660	.840	.830	1.670	1.490	.510	.745	1.255	.085	.415	.204	11.8	.258	.477	.486
7.0	1.680	.820	.840	1.660	1.500	.500	.750	1.250	.090	.410	.220	12.7	.275	.475	.487
7.5	1.691	.809	.845	1.654	1.510	.490	.755	1.245	.090	.409	.221	12.8	.275	.480	.492
8.0	1.700	.800	.850	1.650	1.510	.490	.755	1.245	.095	.405	.234	13.5	.291	.464	.477
8.5	1.705	.795	.853	1.648	1.510	.490	.755	1.245	.098	.403	.243	14.1	.302	.453	.468
9.0	1.710	.790	.855	1.645	1.510	.490	.755	1.245	.100	.400	.250	14.6	.311	.444	.459

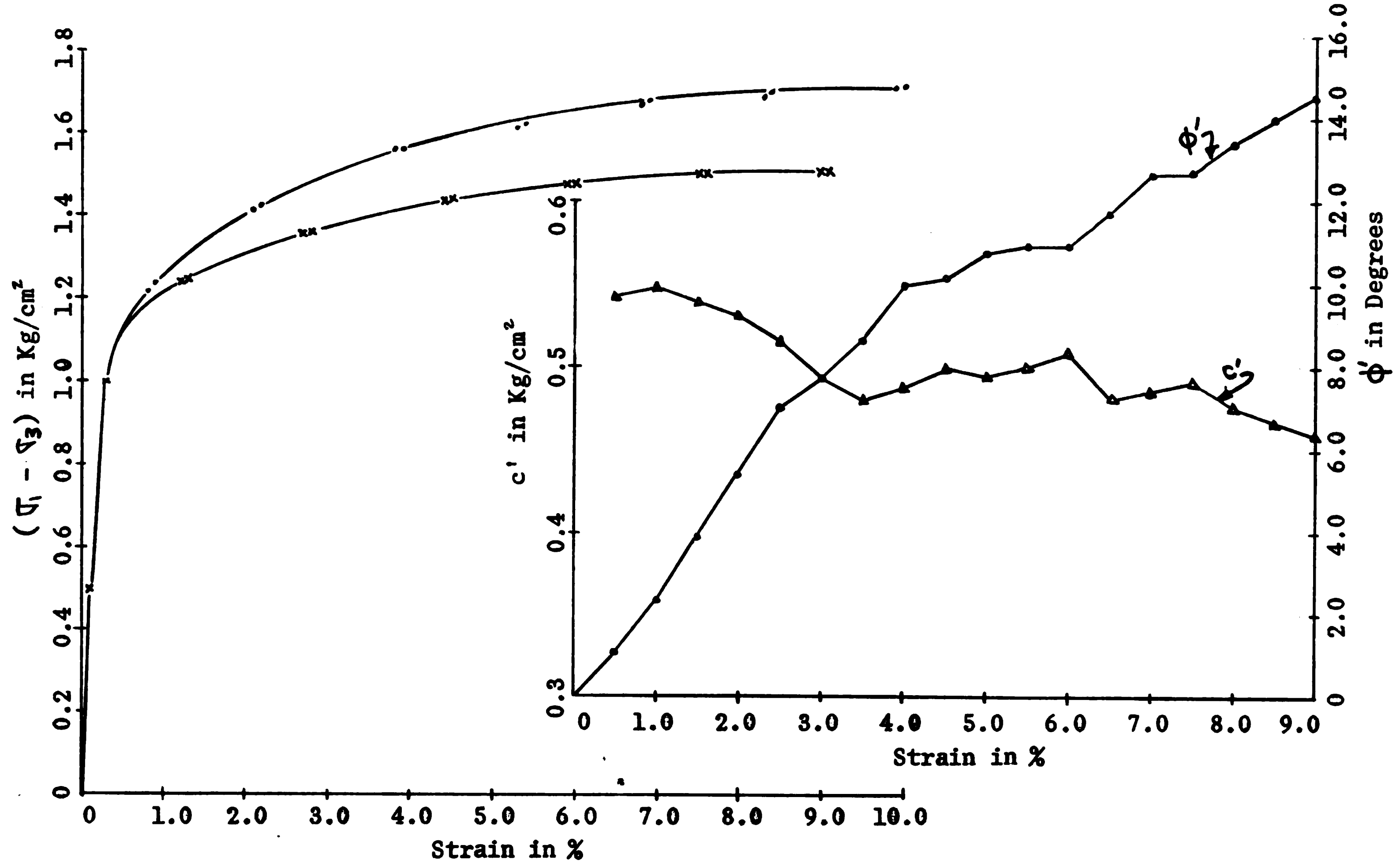

FIGURE 23 - STRESS-STRAIN CURVE FOR TEST F-CFS-1

TABLE 14 - GENERAL DATA SHEET

Date 4/20/63
Operator Holliday
Sample C 7

Test C-C-7 & C-C-CFS-7
Cell 1

TRIMMINGS

Container No. 211

Cont. Wt. 20.34 (grams)

Cont. Wt. & Wet Wt. 46.92

Cont. Wt. & Dry Wt. 39.37

Water Wt. 7.55

Dry Wt. 19.03

Water Content 39.8%

SPECIMEN

Length 3.00 in = 7.62 cm

Area 10.0 cm^2

Volume 76.2 cm^3

	Initial	Final
Wt. of Spec.	137.80	129.15
Dry Wt. of Spec.	97.69	97.69
Wt. of Water	40.11	31.46
Water Content	41.2%	32.2%

TABLE 15 - CONSOLIDATION DATA SHEET

Cell 1
$\Delta V = 12.6\ cm^3$
$L = L_o(V/V_o) = 2.83$ in.
Chamber Pressure 2.00 Kg/cm^2

Test C-C-7 & C-C-CFS-7
$V = V_o - \Delta V = 63.6\ cm^3$
$A = A_o(V/V_o) = 8.87\ cm^2$
Back Pressure 1.5 Kg/cm^2

Date	Time	Elapsed Time Min.	Burette cc	Drainage cc
4/20/63	1014	0.0	10.0	0.0
		.25	8.2	1.8
		.5	8.0	2.0
		1.0	7.7	2.3
		2.0	7.3	2.7
		5.0	6.4	3.6
		13.0	5.0	5.0
		15.0	4.6	5.4
		30.0	2.8---10.0	7.2
	1114	60.0	7.5	9.7
	1214	120.0	5.1---10.0	12.1
	1414	240.0	8.6	13.4
	1714	420.0	8.1	14.0
4/21/63	1035	1461.0	7.6	14.5
	1040	Back Pressure Applied		

TABLE 16 - CREEP DATA SHEET

Cell 1
Chamber Pressure 3.5 Kg/cm²
Dead Load 8.87 Kg

Test C-C-7 & C-C-CFS-7
Back Pressure 1.5 Kg/cm²
$(\sigma_1 - \sigma_3)$ 1.00 Kg/cm²

Date	Elapsed Time Min.	Strain Dial in.	Strain %	Pore Pressure Kg/cm²
4/22/63	0.0	0.0230	0.0	1.52
	.25	.0255	.083	
	.5	.0265	.124	1.90
	1.0	.0275	.159	1.95
	2.0	.0290	.212	2.00
	5.0	.0320	.248	2.08
	10.0	.0351	.427	2.12
	15.0	.0378	.524	2.18
	30.0	.0421	.675	2.25
	60.0	.0481	.886	2.30
	120.0	.0525	1.081	2.35
	240.0	.0559	1.165	2.40
	480.0	.0585	1.259	2.41
	840.0	.0602	1.318	2.47
4/23/63	1440.0	.0610	1.345	2.55
	1740.0	.0615	1.361	2.60
4/24/63	2940.0	.0624	1.394	2.74
	3240.0	.0629	1.415	2.70
4/25/63	4320.0	.0630	1.417	2.86

TABLE 17 - CFS DATA SHEET

Cell 1
Chamber Pressure 3.5 Kg/cm^2
Proving Ring Number 3144
Proving Ring Constant 0.0455 Kg/div.

Test C-C-7 & C-C-CFS-7
Date 4/25/63
*1 Kg Wt. added
**1 Kg Wt. added

$$(\sigma_1 - \sigma_3) - \frac{N(PRC)}{A}(1-\epsilon) = \frac{N(.0455)}{8.87}(1-\epsilon)$$

Time	Load Dial N x 10^{-4}	Strain Dial in.	Strain %	$(\sigma_1 - \sigma_3)$ Kg/cm^2	$\Delta u = 1 - (\sigma_1 - \sigma_3)$ Kg/cm^2	Constant Pressure Cell Kg/cm^2
0853	0.0100	0.040	1.417	1.00	0.0	2.86
0915	.0147	.041	1.451	1.242	.242	2.86
0920	.0149	.042	1.486	1.250	.250	2.86
0951	.0169	.049	1.735	1.348	.348	** 2.36
0955	.0170	.050	1.770	1.353	.353	2.36
1025	.0139	.064	2.265	1.195	.195	* 2.86
1028	.0138	.065	2.300	1.191	.191	2.86
1118	.0159	.078	2.760	1.295	.295	** 2.36
1120	.0160	.079	2.795	1.302	.302	2.36
1152	.0143	.092	3.255	1.216	.216	* 2.86
1153	.0143	.093	3.290	1.216	.216	2.86
1222	.0163	.104	3.675	1.310	.310	** 2.36
1226	.0165	.106	3.745	1.320	.320	2.36
1250	.0149	.118	4.160	1.240	.240	* 2.86
1255	.0148	.120	4.230	1.235	.235	2.86
1326	.0168	.132	4.65	1.332	.332	** 2.36
1332	.0172	.134	4.72	1.352	.352	2.36
1357	.0156	.147	5.20	1.272	.272	* 2.86

TABLE 17 CONTINUED

Cell 1 Test C-C-7 & C-C-CFS-7

Time	Load Dial $N \times 10^{-4}$	Strain Dial in.	Strain %	$(\sigma_1 - \sigma_3)$ Kg/cm^2	$\Delta u = 1 - (\sigma_1 - \sigma_3)$ Kg/cm^2	Constant Pressure Cell Kg/cm^2
1406	.0153	.153	5.4	1.258	.258	2.86
1446	.0181	.167	5.9	1.391	.391	** 2.36
1453	.0184	.170	6.0	1.405	.405	2.36
1520	.0161	.187	6.6	1.288	.288	* 2.86
1526	.0159	.190	6.7	1.284	.284	2.86
1603	.0185	.204	7.2	1.405	.405	** 2.36
1614	.0188	.206	7.3	1.415	.415	2.36
1641	.0163	.223	7.9	1.298	.298	* 2.86
1645	.0162	.226	8.0	1.296	.296	2.86

TABLE 18 - CFS DATA SUMMARY

Upper Curve $\bar{\sigma}_1 = 2.140$

Lower Curve $\bar{\sigma}_1 = 1.640$

Test: C-C-CFS-7

Strain %	$(\sigma_1-\sigma_3)$	$\bar{\sigma}_3$	$\frac{1}{2}(\sigma_1-\sigma_3)$ Y_2	$\frac{1}{2}(\sigma_1+\sigma_3)$ X_2	$(\sigma_1-\sigma_3)$	$\bar{\sigma}_3$	$\frac{1}{2}(\sigma_1-\sigma_3)$ Y_1	$\frac{1}{2}(\sigma_1+\sigma_3)$ X_1	Y_2-Y_1	X_2-X_1	$\tan\alpha = \sin\phi'$	ϕ' Deg.	$X_1\tan\alpha$	$Y_1-X_1\tan\alpha = a = c'\cos\phi'$	c' Kg/cm^2
1.75	1.354	0.786	0.677	1.463	1.230	0.410	0.615	1.025	0.062	0.438	0.142	8.15	0.145	0.470	0.476
2.0	1.342	.798	.671	1.469	1.211	.430	.605	1.035	.066	.434	.152	8.74	.157	.448	.454
2.5	1.320	.820	.660	1.480	1.195	.445	.597	1.042	.063	.438	.144	8.26	.150	.447	.453
3.0	1.305	.835	.653	1.488	1.208	.432	.604	1.036	.049	.439	.111	6.36	.115	.489	.493
3.5	1.314	.826	.657	1.483	1.220	.420	.610	1.030	.047	.436	.108	6.20	.111	.499	.502
4.0	1.325	.815	.663	1.478	1.230	.410	.615	1.025	.048	.430	.112	6.43	.115	.500	.504
4.5	1.340	.800	.670	1.470	1.239	.401	.619	1.020	.051	.450	.113	6.47	.115	.504	.506
5.0	1.360	.780	.680	1.460	1.249	.391	.625	1.016	.055	.444	.124	7.12	.126	.499	.505
5.5	1.380	.760	.690	1.450	1.260	.380	.630	1.010	.060	.440	.135	7.76	.136	.494	.499
6.0	1.405	.735	.703	1.438	1.270	.370	.635	1.005	.068	.544	.157	8.92	.158	.477	.484
6.5	1.411	.729	.705	1.434	1.280	.360	.640	1.000	.065	.434	.150	8.62	.150	.490	.496
7.0	1.416	.724	.708	1.432	1.286	.354	.643	.997	.065	.435	.149	8.59	.149	.494	.500
7.25	1.417	.723	.709	1.432	1.290	.350	.645	.995	.064	.437	.146	8.40	.145	.500	.506

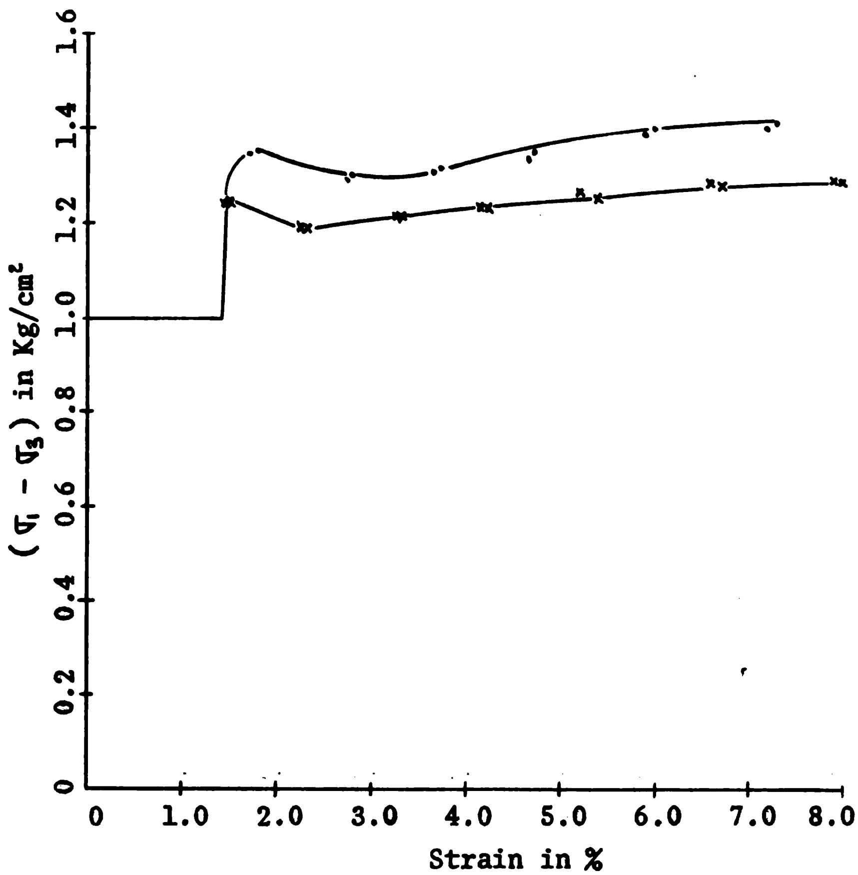

FIGURE 24 - STRESS-STRAIN CURVE FOR C-C-CFS-7

TABLE 19 - GENERAL DATA SHEET

Date 5/20/63
Operator Holliday
Sample F 1

Test F-C-1 & F-C-CFS-1
Cell 1

TRIMMINGS

Container No. 211

Cont. Wt. 20.34 (grams)

Cont. Wt. & Wet Wt. 57.09

Cont. Wt. & Dry Wt. 45.34

Water Wt. 11.75

Dry Wt. 25.00

Water Content 47.0%

SPECIMEN

Length 3.00 in = 7.62 cm

Area 10.0 cm^2

Volume 76.2 cm^3

	Initial	Final
Wt. of Spec.	135.41	120.02
Dry Wt. of Spec.	89.77	89.77
Wt. of Water	45.64	30.25
Water Content	50.9%	33.7%

TABLE 20 - CONSOLIDATION DATA SHEET

Cell 1
$\Delta V = 18.6\ cm^3$
$L = L_o(V/V_o) = 2.73$ in.
Chamber Pressure 2.00 Kg/cm^2

Test F-C-1 & F-C-CFS-1
$V = V_o - \Delta V = 57.6\ cm^3$
$A = A_o(V/V_o) = 8.31\ cm^2$
Back Pressure 1.5 Kg/cm^2

Date	Time	Elapsed Time Min.	Burette cc	Drainage cc
5/20/63	0949	0.0	10.0	0.0
		.25	8.8	1.2
		.50	8.6	1.4
		1.0	8.4	1.6
		2.0	7.8	2.2
		6.0	6.5	3.5
		10.0	5.7	4.3
		15.0	4.3---10.0	5.7
		30.0	7.3	8.4
		60.0	3.1	12.6
		80.0	1.2---10.0	14.5
		132.0	7.5	17.0
	1349	240.0	6.1	18.4
	1549	360.0	5.5---10.0	19.0
	2049	660.0	9.5	19.5
5/21/63	0749	1320.0	9.2	19.8
	0949	1440.0	9.2	19.8
	0955	Back Pressure Applied		

TABLE 21 - CREEP DATA SHEET

Cell 1
Chamber Pressure 3.5 Kg/cm^2
Dead Load 9.56 Kg

Test F-C-1 & F-C-CFS-1
Back Pressure 1.5 Kg/cm^2
$(\sigma_1 - \sigma_3)$ 1.15 Kg/cm^2

Date	Elapsed Time Min.	Strain Dial in.	Strain %	Pore Pressure Kg/cm^2
5/22/63	0.0	0.008	0.0	1.60
	.25	.029	.770	
	.50	.031	.825	2.20
	1.0	.032	.886	2.23
	3.0	.035	.986	2.27
	5.0	.038	1.110	2.32
	10.0	.045	1.364	2.39
	15.0	.048	1.450	2.41
	30.0	.055	1.705	2.50
	60.0	.063	1.995	2.52
	120.0	.070	2.260	2.59
	240.0	.077	2.540	2.62
	360.0	.081	2.677	2.69
	480.0	.083	2.755	2.70
	756.0	.087	2.890	2.76
5/23/63	1440.0	.090	3.010	2.85
	1680.0	.092	3.074	2.88
	1920.0	.093	3.120	2.89
	2160.0	.094	3.150	2.89

TABLE 21 CONTINUED

Cell 1 Test F-C-1 & F-C-CFS-1

Date	Elapsed Time Min.	Strain Dial in.	Strain %	Pore Pressure Kg/cm^2
5/24/63	2880.0	.096	3.220	2.92
	3120.0	.097	3.270	2.98
	3360.0	.099	3.325	2.99
	3600.0	.100	3.350	2.99
5/25/63	4320.0	.102	3.440	3.00
	4560.0	.103	3.490	3.03
	4800.0	.105	3.550	3.05
5/26/63	5760.0	.109	3.700	3.10
	6600.0	.111	3.760	3.10
5/27/63	7200.0	.118	4.01	3.11

TABLE 22 - CFS DATA SHEET

Cell 1
Chamber Pressure 3.5 Kg/cm^2
Proving Ring Number 3144
Proving Ring Constant 0.0455 Kg/div.

Test F-C-1 & F-C-CFS-1
Date 5/27/63
*1 Kg Wt. Added
**1 Kg Wt. Removed

$$(\sigma_1 - \sigma_3) - \frac{N(PRC)}{A}(1-\epsilon) = \frac{N(.0455)}{8.31}(1-\epsilon)$$

Time	Load Dial N x 10^{-4}	Strain Dial in.	Strain %	$(\sigma_1 - \sigma_3)$ Kg/cm^2	$\Delta u = 1.15 - (\sigma_1 - \sigma_3)$ Kg/cm^2	Constant Pressure Cell Kg/cm^2
0815	0.0100	0.109	4.01	1.150	0.0	3.11
0841	.0125	.112	4.11	1.281	.131	3.11
0843	.0125	.113	4.14	1.281	.131	3.11
0845	.0125	.114	4.175	1.281	.131	3.11
0928	.0147	.127	4.64	1.398	.248	** 2.61
0931	.0148	.128	4.68	1.400	.250	2.61
1007	.0114	.145	5.30	1.223	.073	* 3.11
1009	.0114	.146	5.33	1.222	.072	3.11
1150	.0152	.180	6.59	1.416	.266	** 2.61
1152	.0152	.181	6.63	1.416	.266	2.61
1155	.0152	.182	6.66	1.416	.266	2.61
1318	.0116	.219	8.02	1.231	.081	* 3.11
1320	.0116	.220	8.06	1.228	.078	3.11
1420	.0150	.240	8.77	1.400	.250	** 2.61
1422	.0151	.241	8.80	1.405	.255	2.61
1448	.0118	.254	9.30	1.242	.092	* 3.11
1454	.0117	.256	9.40	1.234	.084	3.11
1500	.0117	.259	9.50	1.232	.082	3.11

TABLE 23 - CFS DATA SUMMARY

Upper Curve $\bar{\sigma}_1 = 2.040$ | Lower Curve $\bar{\sigma}_1 = 1.540$ | Test: F-C-CFS-1

Strain %	$(\bar{\sigma}_1-\bar{\sigma}_3)$	$\bar{\sigma}_3$	$\frac{1}{2}(\bar{\sigma}_1-\bar{\sigma}_3)$ Y_2	$\frac{1}{2}(\bar{\sigma}_1+\bar{\sigma}_3)$ X_2	$(\bar{\sigma}_1-\bar{\sigma}_3)$	$\bar{\sigma}_3$	$\frac{1}{2}(\bar{\sigma}_1-\bar{\sigma}_3)$ Y_1	$\frac{1}{2}(\bar{\sigma}_1+\bar{\sigma}_3)$ X_1	Y_2-Y_1	X_2-X_1	$\tan\alpha = \sin\phi'$	ϕ' Deg.	$X_1\tan\alpha$	$Y_1-X_1\tan\alpha = a = c'\cos\phi'$	c' Kg/cm^2
4.25	1.440	0.600	0.720	1.320	1.270	0.270	0.635	0.905	0.085	0.415	0.205	11.8	0.186	0.449	0.458
4.5	1.410	.630	.705	1.335	1.235	.305	.617	.922	.088	.413	.212	12.2	.195	.422	.432
5.0	1.401	.639	.701	1.340	1.225	.315	.613	.928	.088	.412	.214	12.3	.198	.415	.425
5.5	1.405	.635	.703	1.338	1.224	.316	.612	.928	.091	.410	.222	12.8	.206	.406	.417
6.0	1.410	.630	.705	1.335	1.225	.315	.613	.928	.092	.407	.226	13.1	.209	.404	.415
6.5	1.412	.628	.706	1.334	1.225	.315	.613	.928	.093	.406	.229	13.2	.212	.401	.412
7.0	1.410	.630	.705	1.335	1.228	.312	.614	.926	.091	.409	.223	12.9	.206	.408	.419
7.5	1.410	.630	.705	1.335	1.229	.311	.615	.926	.090	.409	.220	12.7	.204	.411	.422
8.0	1.408	.632	.704	1.336	1.230	.310	.615	.925	.089	.411	.216	12.5	.200	.415	.426
8.5	1.405	.635	.703	1.338	1.230	.310	.615	.925	.088	.413	.213	12.3	.197	.418	.429
9.0	1.403	.637	.701	1.338	1.230	.310	.615	.925	.086	.413	.208	12.0	.192	.423	.433

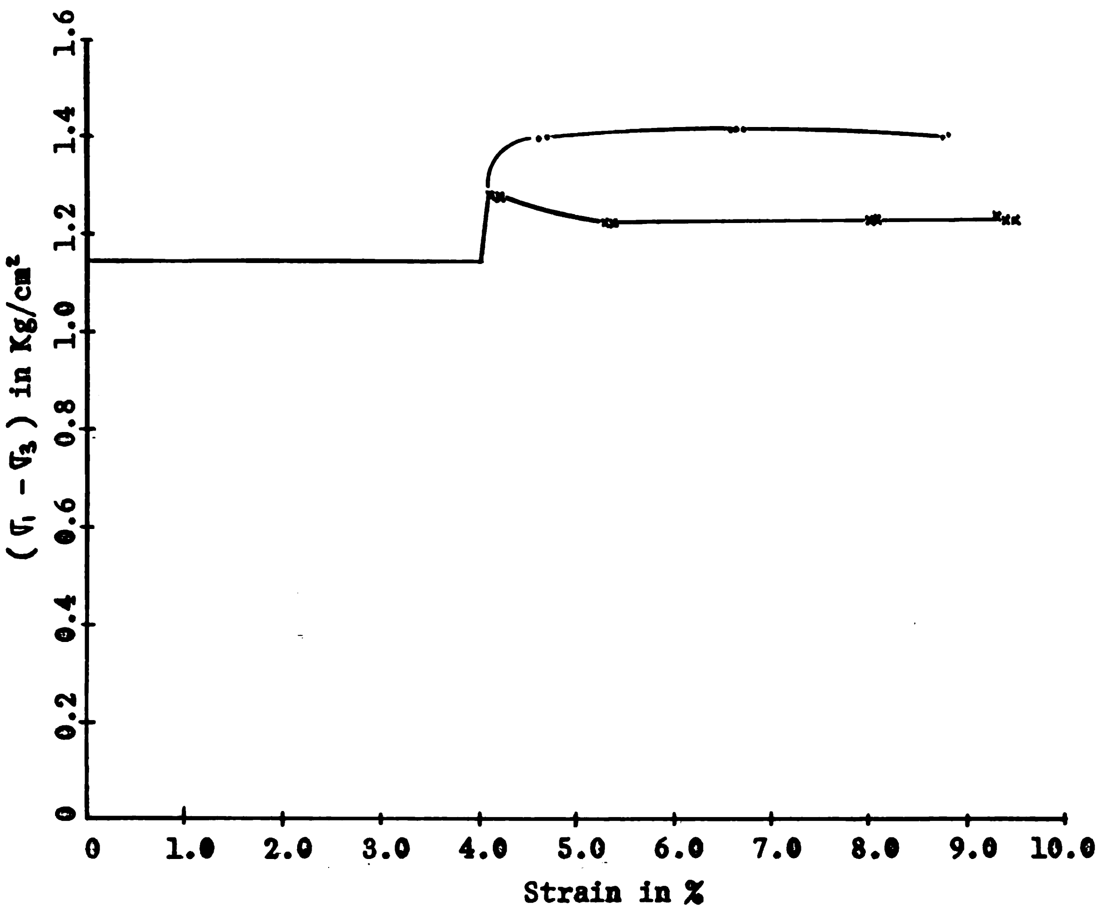

FIGURE 25 - STRESS-STRAIN CURVE FOR F-C-CFS-1

7.3 Calculations for τ_ϕ and c' for Compacted Clay

a) Creep Test (C-C-7)

$2K = \sigma_1 - \sigma_3 = 1.00$ Kg/cm^2

Threshold shear strain $= \gamma_T = 0.0\%$

Threshold shear stress $= \tau_T = 0.35$ Kg/cm^2

$\tau_K = K - \tau_T = \left(\frac{\sigma_1 - \sigma_3}{2}\right) - \tau_T = \frac{1.00}{2} - 0.35 = 0.15$ Kg/cm^2

From equation (3.4-1)

$$G = \frac{\tau_K}{\gamma_F} = \frac{0.15}{0.015} = 10 \text{ Kg/cm}^2$$

From equations (2.3-1) and (2.3-3)

$$\tau_\phi = G\gamma_j$$

$$\tau_c = \tau_K - \tau_\phi$$

From Figure 14

$\gamma_1 = 9.25 \times 10^{-3}$	$t_1 = 60$ min
$\gamma_2 = 10.9 \times 10^{-3}$	$t_2 = 125$
$\gamma_3 = 12.5 \times 10^{-3}$	$t_3 = 460$
$\gamma_4 = 13.1 \times 10^{-3}$	$t_4 = 825$
$\gamma_5 = 14.2 \times 10^{-3}$	$t_5 = 4320$

Increment j	$\tau_\phi = G\gamma_j$	$\tau_c = \tau_K - \tau_\phi$	$c' = \tau_T + \tau_c$
1	0.093	0.057	0.407
2	.109	.041	.391
3	.125	.025	.375
4	.131	.019	.369
5	.142	.008	.358

b) Creep-CFS Test

Y_1	c'	$\tau_\phi = Y_1 - c'$	Creep phase Time in min.
0.500	0.469	0.031	120
.500	.422	.078	480
.500	.372	.128	960
.500	.376	.124	1440
.500	.356	.144	4320

7.4 Calculations for τ_ϕ and c' for Consolidated Clay

a) Creep Test (F-C-1)

$2K = \sigma_1 - \sigma_3 = 1.15 \text{ Kg/cm}^2$

Threshold shear strain $= \gamma_T = 0.0\%$.

Threshold shear stress $= \tau_T = 0.370 \text{ Kg/cm}^2$

$\gamma_F = \epsilon_F = 4.0\%$

$\tau_K = K - \tau_T = \left(\frac{\sigma_1 - \sigma_3}{2}\right) - \tau_T = \frac{1.15}{2} - .037 = 0.205 \text{ Kg/cm}^2$

From equation (3.4-1)

$$G = \frac{\tau_K}{\gamma_F} = \frac{0.205}{0.04} = 5.13 \text{ Kg/cm}^2$$

From equations (2.3-1) and (2.3-3)

$$\tau_\phi = G\gamma_j$$

$$\tau_c = \tau_K - \tau_\phi$$

From Figure 15

$\gamma_1 = 1.75 \times 10^{-2}$	$t_1 = 30$ min.
$\gamma_2 = 2.24 \times 10^{-2}$	$t_2 = 125$
$\gamma_3 = 2.55 \times 10^{-2}$	$t_3 = 250$
$\gamma_4 = 2.87 \times 10^{-2}$	$t_4 = 500$
$\gamma_5 = 3.40 \times 10^{-2}$	$t_5 = 7200$

Increment j	$\tau_\phi = G\gamma_j$	$\tau_c = \tau_K - \tau_\phi$	$c' = \tau_T + \tau_c$
1	0.0899	0.115	0.485
2	.1155	.089	.459
3	.1310	.074	.444
4	.1475	.058	.428
5	.1745	.031	.401

b) Creep-CFS Test

Y_1	c'	$\tau_\phi = Y_1 - c'$	Creep phase Time in min.
0.575	0.564	0.011	60
.575	.420	.155	240
.575	.393	.182	1440
.575	.379	.196	7200

7.5 Sample Calculations for Extrapolation of c' from Creep-CFS Test

Test C-C-CFS-7

$2K = (\sigma_1 - \sigma_3) = 1.00$ Kg/cm^2

Extrapolated $\phi' = 7.4^\circ$

Constant effective stress $\bar{\sigma}_1 = 1.640$ Kg/cm^2

Effective radial stress at end creep = 0.640 Kg/cm^2

$X_1 = 1/2\ (1.00) + 0.640 = 1.140$

$Y_1 = 1/2\ (1.00) = 0.500$

$\sin 7.4^\circ = 0.129 = \tan\alpha$

$X_1 \tan\alpha = 0.147$

$a = 0.500 - 0.147 - 0.353$

$c' = 0.353/\cos 7.4^\circ = 0.356$ Kg/cm^2